SUPPLEMENTAL MATERIAL.

SUPPLEMENTAL METHODS

Human Fibroblast Cells Isolation and Reprogramming

Fresh skin biopsies from patients were cut into small pieces (less than 1 mm^3) and incubated with collagenase 1 (1 mg/ml in DMEM) at 37°C for 8 hours. The digested tissue from each patient was placed on tissue culture a dish, covered with a glass coverslip, and cultured in DMEM containing 10% FBS. After 7 days with daily media changes, fibroblast outgrowths on the tissue culture dish and coverslip were passaged. Fibroblasts were reprogrammed before passage 5 though episomal transfection with OCT4, SOX2, KLF4 and OCT4 expression constructs using Nucleofector™ Kits for Human Dermal Fibroblasts (Lonza). iPSCs were tested for pluripotency by RTqPCR and immunostaining of pluripotency genes, karyotyping, and *in vivo* teratoma formation.

Human iPSC Maintenance and Genome Editing

All the IPSC lines in study were maintained in mTeSR1 medium (STEMCELL Technologies) and passaged in versene solution (15040066, Thermo Fisher Scientific) every five days. Culture dishes were pre-coated with Matrigel (hESC-Qualified Matrix, LDEV-Free, Corning) diluted 1:100.

The procedures for CRISPR/Cas9 genome editing were described in detail in a recent publication[1]. We started with wild-type PGP1 human iPSCs that contained doxycycline-inducible Cas9. Plasmid expressing guide RNA and 90 nt donor oligonucleotide was transfected into the PGP1-Cas9 cells with the Human Stem Cell Nucleofector Kit (Lonza #VPH-5012) using program B-016. Candidate clones from genome editing were PCR amplified and sequenced using the following primer pairs: Site R4651, R4651-F: TTGTAAGTTTACGTGGCAGGA and R4651-R: CGCGTGCATATGTGTGTGTA; Site S2814, S2814-F: ACACTATGTTTGGAAATTTGTGCCA and S2814-R: TGCTTTCCTGCATATATTTGGCA; Site S2808, S2808-F: GGGCTGGAGAATTGAAAGAAC and S2808-R: CCCTTCTAAATTTTGTGACTCTTCA. R4651I heterozygous and S2814A and S2808A homozygous mutants were retained.

Guide RNA sequences were:

Site 358: GAACATCTGAAATAAAATACGG

Site 2808: CGTATTTCTCAGACAAGCCAGG

Site 2814: CAAATGATCTAGGTTTCTGTGG

Site 4651: GACAAATTTGTTAAAATAAAGG

Single stranded oligonucleotide HDR template were:

Site 358:

GAAAAGAAGTAGATGGCATGGGAACATCTGAAATAAAATACGGTAACTCAGTATGCTATATACAACATGTAGACACAGGCCTATGGCTTA

Site 2808:

CGGGAGGGAGACAGCATGGCCCTTTACAACCGGACTCGTCGTATTGCTCAGACAAGCCAGGTAAGAATTCATCACGGTGATGAATCAACTG

Site 2814:

AGGTTTTTAATGAGGCACTGTTTTTTCACACAAATGATCTAGGTTGCTGTGGACGCTGCCCATGGTTACAGTCCCCGGGCCATTGACATGA

Site 4651:

ATTTTAGGTCATTTCCCAACAACTACTGGGACAAATTTGTTAAAATAAAGGTAATATTACTTGGAATCCTCTACATTTTTCTTAAAGCACA

We predicted Cas9-gRNA off-target sites using http://crispr.mit.edu/ [2]. Amplicons containing the top 10 predicted sites were amplified from iPSCs and Sanger sequenced.

Differentiation to iPSC-CMs

Human iPSCs were seeded onto Matrigel-coated dishes at normal passage density. iPSC differentiation to iPSC-CMs followed the timeline shown in Figure VE in the online-only Data Supplement. On day 3 of iPSC culture, mTeSR1 medium was removed, cells were rinsed once with PBS (without Ca^{2+} or Mg^{2+}), and cultured in Differentiation Medium (RPMI medium (11875093, Thermo Fisher Scientific) with B27 without insulin (A1895601, Thermo Fisher Scientific)) containing 5 μM CHIR99021 (72054, STEMCELL Technologies). After 24 hours, medium was changed to differentiation medium without CHIR99021. At differentiation day 3, cells were cultured in differentiation medium containing 5 μM IWR-1 (3532, Tocris). After 48 hours, cells were cultured in differentiation medium without IWR until day 15, with media changes every 2-3 days. At day 15, the

cells were cultured in Selection Medium (Non-Glucose DMEM (11966025, Thermo Fisher Scientific) with 0.4 mM Lactate (# L7022, Sigma Aldrich)) for 3-5 days to enrich for iPSC-CMs [3]. To create the seeding solution for the opto-MTF, iPSC-CMs were isolated after lactate selection by incubating in collagenase 1 (Sigma C-0130, 100mg collagenase 1 in 50 ml PBS/20% FBS) for 1 hour, followed by a 0.25% Trypsin incubation at 37°C for 5-10 mins. 50% FBS in DMEM with 50 µg/ml DNase I (# 260913, EMD Millipore) was used to stop trypsinization. The iPSC-CMs were suspended in Culture Medium (RPMI:Non-Glucose DMEM 1:1, plus 1x B27 without insulin and 0.2 mM Lactate) containing 10% FBS and 10 µM Y27632.

Culture of Commercial Human Stem Cell-Derived Cardiomyocytes

Commercial human stem cell-derived cardiomyocytes (Cor4U; Axiogenesis, Cologne, Germany) were cultured according to manufacturer's instructions. Briefly, a T-25 cell culture flask (per each 1-million cryovial) was coated with 0.01 µg/mL fibronectin (FN) (BD Biosciences, Bedford, MA) one day before the cell seeding. Cryovials were quickly thawed in a 37°C water bath and resuspended in 9 mL of complete culture media (Axiogenesis, Cologne, Germany) supplemented with 4.5 µL of 10 mg/mL puromycin (Axiogenesis, Cologne, Germany). After 24 hours, the cell culture media were replaced with puromycin free media (total volume 10 ml). After 48 hours, we created the seeding solution by dissociating cells with 0.25% trypsin-EDTA (Life Technologies). The Cor4U cells were suspended in puromycin free media.

Neonatal Rat Ventricular Myocyte Culture

Animal procedures were performed under protocols approved by Harvard University's Institutional Animal Care and Use Committee. Preparation of neonatal rat ventricular myocytes was described previously[4]. Briefly, ventricles were removed from 2 day old Sprague Dawley rat pups (Charles River Laboratories). The tissue was manually minced. For the first enzymatic digestion, the tissue was placed in a 0.1% trypsin (Sigma Aldrich) solution at 4°C for approximately 12 hours. For the second stage of enzymatic digestion, the trypsin was replaced with a 0.1% type II collagenase (Sigma Aldrich) solution. After four iterations of the second stage digestions at 37°C, ventricular myocytes were further isolated from the resulting dissociated cell solution by centrifuging and passing the resuspended solution through a 40 µm cell strainer. The solution was pre-plated twice for 45 minutes each at 37°C to remove fibroblasts and endothelial cells. Then, we created the seeding

solution by resuspending the resulting ventricular myocytes in a M199 cell media (Life Technologies) supplemented with 10% heat-inactivated FBS (Life Technologies).

Gelatin Muscular Thin Film (MTF) Substrate Fabrication

Glass coverslips (22 by 22 mm square) were cleaned using 70% ethanol (Sigma) and were then covered with low-adhesive tape (3M). Using a laser engraving system (Epilog Laser), the tape was cut to have two rectangles in the center, surrounded by four trapezoids on the outer edges. The inner rectangles of 3 mm by 10 mm and 7 mm by 10 mm are for the cantilever and base region of the MTFs respectively (Figure VIM in the online-only Data Supplement).

Glass coverslips were selectively activated, such that the gelatin in the base region of MTFs would firmly attach to the glass coverslips but the gelatin in the cantilever region would be easily peeled. Firstly, only the base region tape was removed, while the tapes in the cantilever and outer regions remained to protect the glass from the following activation. The coverslips were activated with a 0.1 M NaOH (Sigma) solution for 5 minutes, a 0.5% APTES (Sigma) solution in 95% ethanol (Sigma) for 5 minutes, followed by a 0.5% glutaraldehyde solution for 30 minutes.

The tape in the cantilever region was removed after the activation process, but the tapes in outer regions remained on the glass coverslips. 20% w/v gelatin (Sigma) and 8% w/v MTG (Ajinomoto) were warmed to 65°C and 37°C, respectively for 30 minutes. Then, the solutions were mixed to produce a final solution of 10% w/v gelatin and 4% w/v MTG. 300 µl of the gelatin mixture was quickly pipetted onto the exposed inner rectangle regions of glass coverslips. PDMS stamps with line groove features (25 µm ridge width, 4 µm groove width, and 5 µm groove depth) were then inverted on top of the gelatin drop and weight was applied using a 200 g weight. Gelatin was then left to cure overnight at room temperature with the stamp and the weight in place.

After the gelatin cured, the weight was carefully removed along with excess gelatin on the sides of the stamp. To minimize damage to the micro-molded gelatin, the coverslip and stamp were immersed in distilled water to re-hydrate the gelatin for an hour. The stamp was then carefully peeled off the gelatin.

Coverslips with the micro-molded gelatin were quickly dried with paper wipes (Kimwipes, Kimberly-Clark Professional). Cantilevers (1 mm wide × 2 mm long) were laser engraved into the dehydrated micro-molded

gelatin using an Epilog laser engraving system with 3% power, 7% speed, and a frequency of 1900 Hz. Gelatin chips were UVO-treated for 90 seconds and re-hydrated in a 2 mM MES solution of pH 4.5 with 1 mg/ml collagen and 0.1 mg/mg fibronectin. The gelatin chips were stored in solution at room temperature for 2 hours. The collagen and fibronectin solution was replaced with PBS. The gelatin chips were stored at 4ºC until cell seeding.

Soft Lithography and PDMS Micromolded Stamp Fabrication.

Micro-molded stamps were fabricated from polydimethylsiloxane (PDMS, Sylgard 184, Dow Corning) using previously published soft lithography protocols [4,5]. Briefly, 5 µm thick SU-8 2005 photoresist (MicroChem) was spin-coated on silicon wafers and prebaked at 90°C as suggested in the MicroChem protocol manual. The SU-8 layer was exposed to UV light under customized photomasks with line features (25 µm wide dark lines and 4 µm wide clear lines). After exposure, wafers were post-baked at 90°C, developed with propylene glycol monomethyl ether acetate, and silanized with fluorosilane (United Chemical Technologies). PDMS was mixed at 10:1 base to curing agent ratio, poured onto the wafer, cured at 65°C for 4 hours, carefully peeled from the wafer, and cut into micromolded stamps.

Opto-MTF Construction

ChR2 lentiviral vector in which the cardiac troponin T promoter drives ChR2-eYFPP was constructed based on the FCK(1.3)GW plasmid with the cardiac troponin T (cTnT) promoter, ChR2, and enhanced yellow fluorescent tag [6,7]**.**

After 15 days of differentiation and 3-5 days of lactate selection, WT, CPVT1p, CPVT1e, and CPVT2e iPSC-CMs were suspended in culture medium media containing 10% FBS and 10 µM Y27632, as described in **Differentiation to iPSC-CMs**. After 3 days culture in the plate, commercial human stem cell-derived cardiomyocytes (Cor4U; Axiogenesis, Cologne, Germany) were suspended in puromycin free Cor4U media as described in **Culture of Commercial Human Stem Cell-Derived Cardiomyocytes**. NRVMs were harvested and suspended in a M199 cell media (Life Technologies) supplemented with 10% heat-inactivated FBS (Life Technologies) as described in **Neonatal Rat Ventricular Myocyte Culture**. Prior to seeding, the gelatin chips were washed with PBS and incubated with hiPSC-CM, Cor4U, or NRVM seeding media. Dissociated hiPSC-CMs were seeded on opto-MTFs at a final concentration of 1 million cells per 600 µl. 48 hours after seeding on

opto-MTFs, the culture media was replaced with Chip Culture Medium (1:1 mix of Culture Medium and Selection Medium). At the same time, the iPSC-CMs were transduced with ChR2 lentivirus at a multiplicity of infection of 14-23 for 24 hours. Commercial Cor4U cells and NRVM cells were seeded onto devices at a density of 220 k/cm^2 and 110 k/cm^2, respectively. After 24 hours, the NRVMs were treated with ChR2 lentivirus at multiplicity of infection of 14-23 for 24 hours. Recordings were made from opto-MTF chips 5-7 days after seeding.

Immunofluorescence Staining of iPSC-CMs

Differentiated cardiomyocytes were seeded on Matrigel-coated glass bottom dishes for 5 days. The cells were fixed by 4% paraformaldehyde for 10 min at room temperature, washed with PBS, and then blocked and permeabilized with 5% donkey serum plus 0.02% Triton X-100 at 4°C overnight. The primary antibodies were used at 1:200 at 4°C for >8 h. Primary antibodies were: Oct4 (Santa Cruz, SC8628), SSEA4 (Millipore, MAB4304), Cardiac Troponin I (Abcam, ab56357), ACTN2 (Abcam, ab56357), RYR2 (Abcam, ab2827). After washing, dishes were incubated with Alexa Donkey secondary antibodies (Life Technologies). Imaging was performed on an Olympus FV1000 confocal microscope.

Immunofluorescent Staining of Engineered Cardiac Tissues on Micromolded Gelatin Hydrogels

iPSC-CM opto-MTFs were washed with PBS at 37°C, fixed in PBS with 4% paraformaldehyde and 0.05% Triton X-100 for 12 mins at 37°C, and rinsed with PBS. Tissues were stained with mouse anti-sarcomeric α-actinin monoclonal primary antibody (Sigma) for 1 hour at room temperature, and then with a secondary antibody against mouse IgG conjugated to Alexa-Fluor 546 (Life Technologies) and DAPI (Life Technologies). The samples were mounted on glass slides with ProLong Gold antifade mountant (Life Technologies). Z-stack images were acquired using a confocal microscope (Zeiss LSM) equipped with an alpha Plan-Apochromat 100x/1.46 Oil DIC M27 objective.

Western Blot

10% Invitrogen Bolt gels were used to run all the samples. For RYR2 and RYR2-P2814 western blots, transfer was performed using 75V for 900 minutes. Other westerns were transferred using 80V for 120 min. The antibody antibodies used for western blots were are as follows: CaMKII-phospho-T286 (Abcam, ab171095), CaMKII (Abcam, ab134041), RYR2-phospho-S2814 (Badrilla A010-31AP), and Cardiac Troponin T (Abcam

ab45932). HiMark Pre-Stained Protein Standards (Life Technologies #LC5699) was used as molecular weight markers.

Calcium Imaging of Cell Clusters

After 15 days of differentiation and 3-5 days of lactate selection, iPSC-CMs were seeded on Matrigel-coated glass bottom dishes with Chip Culture Medium (1:1 mix of Culture Medium and Selection Medium) for 5-7 days. 50 µg of Fluo-4 (F14201, Thermo Fisher Scientific) was dissolved in 8 µl of DMSO, then diluted 1:1 with Pluronic® F-127 (20% Solution in DMSO) (P3000MP, Thermo Fisher Scientific). The iPSC-CMs were treated with 3 µg/ml Fluo-4 at 37°C for a half hour. Alternatively, cells were loaded with FluoVolt (1 µM, Thermo Fisher Scientific) and Rhod4 (1 µM, Thermo Fisher Scientific). The samples were then washed with Chip Culture Medium before Ca^{2+} imaging on an Olympus FV1000 using line scan mode (10 msec/line, 1000 lines per recording). The scan line was positioned within individual iPSC-CMs that belonged to clusters of 3-10 cells. Recordings of Ca^{2+} sparks and spontaneous Ca^{2+} release events were made during periods when cells did not exhibit spontaneous Ca^{2+} transients and during periods of spontaneous beating, respectively. 0.025 µM myristoylated Autocamtide-2-related Inhibitory Peptide (AIP; SCP0001 Sigma) and myristoylated 1 µM PKA Inhibitor 14-22 amide (476485, EMD Millipore) were used as CaMKII and PKA inhibiting peptides. Isoproterenol and dantrolene were each used at 1 µM.

Optical Setup for opto-MTF

We modified the tandem-lens macroscope (Scimedia) for simultaneous Ca^{2+} imaging and contractility measurement with optogenetic stimulation (Figure II in the online-only Data Supplement). For Ca^{2+} imaging, the system was equipped with a high-speed camera (MiCAM Ultima, Scimedia), a plan APO 1× objective, a collimator (Lumencor) and a 200 mW mercury lamp for epifluorescence illumination (X-Cite exacte, Lumen Dynamics). For contractility measurements, a high-spatial resolution sCMOS camera (pco.edge, PCO AG) and 880 nm darkfield LED light (Advanced Illumination) were incorporated into the system. The field of view of the system for Ca^{2+} and dark field imaging was 10 mm by 10 mm and 16 mm by 13 mm, respectively. For optogenetic stimulation, an 8 channel LED array (465/25 nm, Doric Lenses) was used to generate optical pulses. Light pulses for pacing individual MTFs were delivered through the 8 optical fibers (400 µm diameter, NA 0.48, Doric Lenses) and 8 mono fiber optic cannulas (flat end, 400 µm diameter, NA 0.48, Doric Lenses) mounted 500

μm above the gelatin chips using a 3-axis manipulator (Zaber, Canada). To prevent overlap of the excitation light wavelength for Ca^{2+} transients and dark field illumination for contractility measurements with the ChR2 excitation wavelength, we used a filter set with longer wavelengths than the ChR2 excitation wavelength. For Ca^{2+} imaging, we used an excitation filter with 580/14 nm, a dichroic mirror with 593 nm cut-off, and an emission filter with 641/75 nm (Semrock, Rochester, NY). For dark field imaging, we added a dichroic mirror with 685 nm cut-off and long pass emission filter with 664 nm cut-off (Semrock, Rochester, NY) into the light path of Ca^{2+} imaging. The light sources of the LED array were independently controlled by analog signals that were synthesized with an analog output module (NI 9264, National Instruments) by custom software written in LabVIEW (National Instruments). For post-imaging processing, these analog signals were recorded using a high-speed camera and a high-spatial resolution sCMOS camera simultaneously, to use the analog signals as a reference for aligning frames from both systems.

Tissue Level Data Acquisition

At post-transduction day 3, engineered opto-MTF tissues were incubated with 2 μM X-Rhod-1 (Invitrogen, Carlsbad, CA) for 30 min at 37°C, rinsed with culture medium with 2% FBS to remove nonspecifically associated dye, and incubated again for 30 mins to complete de-esterification of the dye. Prior to recording for the experiments, the culture media was replaced with Tyrode's solution (1.8 mM $CaCl_2$, 5 mM glucose, 5 mM Hepes, 1 mM $MgCl_2$, 5.4 mM KCl, 135 mM NaCl, and 0.33 mM NaH_2PO_4 in deionized water, pH 7.4, at 37°C; Sigma). The engineered tissue sample in Tyrode's solution was maintained at 37°C during the experiments using a culture dish incubator (Warner Instruments).

The engineered opto-MTF tissues were stimulated with an optical pulse of 10 ms over a range of frequencies from 0.7 to 3 Hz using a custom LabVIEW program (National Instruments). The optical point stimulation was applied at one end of the MTF tissue using an LED light source (465/25 nm, Doric Lenses). For each recording, Ca^{2+} and dark field images were simultaneously acquired with 2000 frames and 400 frames at a frame rate of 200 Hz and 100 Hz over 10 s and 4 s, respectively.

Engineered opto-MTF tissues were treated with 6 μM dantrolene or 2 μM AIP (both from Sigma-Aldrich). Dantrolene was added in Tyrode's solution after calcium indicator (X-Rhod-1) incubation and at least 10 mins before recording. AIP was added in culture medium at least 15 mins before calcium indicator (X-Rhod-1)

incubation (30 mins) and de-esterification (30 mins), in order to ensure at least 1-hr AIP incubation before recording.

Analysis of Calcium Imaging Data

Post-processing of the raw calcium data was conducted with custom software written in MATLAB (MathWorks). A spatial filter of 3 × 3 pixels was applied to improve the signal-noise ratio. First, local Ca^{2+} activation time, $T_{act\ p,\ px}$ and 80% repolarization time, $CaTD80_{p,\ px}$ of each pixel (px) and each pulse (p) was calculated by identifying the time with the maximum upstroke slope and the time from the upstroke to 80% recovery, respectively. Then, the calcium propagation speed, $CaS_{p,\ px}$ of each pixel and each pulse was determined by calculating the x- and y-directional change rate of $T_{act\ p,\ px}$ in 21 pixels (3 pixels in the transverse direction, x, and 7 pixels in the longitudinal direction of the wave, y). To calculate the spatial dispersions of the Ca^{2+} propagation speed, CaS_{spat} and 80% repolarization time, $CaTD80_{spat}$, we averaged $CaS_{p,\ px}$ and $CaTD80_{p,\ px}$ over multiple consecutive pulses (3 - 20 pulses) of each pixel and calculated the coefficient of variance of these temporal averages over an area of interest (500 to 1000 pixels). To calculate the temporal dispersions of calcium propagation speeds, CaS_{temp} and 80% repolarization time, $CaTD80_{temp}$, we averaged $CaS_{p,\ px}$ and $CaTD80_{p,\ px}$ over all areas of interest of each pulse and calculated the coefficient of variance of these spatial averages over multiple consecutive pulses. The global Ca^{2+} propagation speed, CaS_{global} and 80% repolarization time, $CaTD80_{global}$, were calculated by averaging $CaS_{p,\ px}$ and $CaTD80_{p,\ px}$ over multiple consecutive pulses and pixel areas of interest. Regions where local Ca^{2+} propagation speed was less than 0.2 cm/s were defined as having functional conduction block. In addition, we measured global Ca^{2+} wavelength, Ca^{2+} signal amplitude, and relative diastolic Ca^{2+} level. The global calcium wavelength was defined as the distance traveled by the waves during the duration of the calcium refractory period and calculated by multiplying calcium propagation speed, CaS_{global} and 80% repolarization time, $CaTD80_{global}$. The calcium amplitude was calculated as a difference between peak systolic and diastolic Ca^{2+} level. Relative diastolic Ca^{2+} levels were calculated from the mean diastolic value at more than 500 sampling points distributed throughout the tissue by subtracting the background intensity measured at 10 points outside the opto-MTF. This background-subtracted value at the base rate (0.7 Hz, no ISO) was set as F_0. The change in relative diastolic Ca^{2+} level at higher pacing frequencies was calculated as $(F-F_0)/F_0$. To determine the

ISO and pacing frequency-dependence of global variables, global variable data were normalized to values from the same opto-MTF at 1.5 Hz pacing without ISO.

Analysis of Contractility Dark Field Imaging Data.

Post-processing of the dark field imaging data was conducted using custom software written in MATLAB (MathWorks). We modified the contractile stress quantification ImageJ software program that was previously published from our group [4,8]. First, we measured the projected length of each MTF from each frame by using image thresholding MATLAB functions. Then, we calculated the film stress using the projected length, gelatin film thickness, and gelatin properties by considering the geometric relationship of the radius of curvature, the angle of the arc, and the projected length of the film, using a modified Stoney's equation [4]. Here, we used Young's modulus = 56 kPa, and gelatin MTF thickness = 188 μm, as previously determined by our group [9]. Twitch stress was calculated as the difference between peak and baseline stresses.

Supplemental Table 1. Observed Reentry Initiation Events

For a subset of reentrant arrhythmias that occurred, the initiation of the arrhythmia was recorded in 8 cases. These fell within two classes. At lower pacing rates and in the absence of β-adrenergic stimulation, spontaneous Ca^{2+} waves that arose from the edges of tissues collided with paced Ca^{2+} waves. At higher pacing rates, regional conduction block associated with localized Ca^{2+} transient abnormalities initiated reentry.

Tissue type	Pacing freq. (Hz)	β-adrenergic stimulation	Reentry initiation mechanism	Note
CPVT1p	0.7	No	Spontaneous Ca^{2+} waves intersecting with paced Ca^{2+} waves	
CPVT1p	1.5	No	Spontaneous Ca^{2+} waves intersecting with paced Ca^{2+} waves	
CPVT1p	1.5	No	Spontaneous Ca^{2+} waves intersecting with paced Ca^{2+} waves	Supplemental Video 10 Supplemental Figure 16
CPVT1p	3	No	Regional conduction block caused by localized Ca^{2+} transient abnormalities	
CPVT1p	3	ISO (10 μM)	Regional conduction block caused by localized Ca^{2+} transient abnormalities	Supplemental Video 13 Figure 4
CPVT1p	3	ISO (10 μM)	Regional conduction block caused by localized Ca^{2+} transient abnormalities	
CPVT1e	2.5	No	Regional conduction block caused by localized Ca^{2+} transient abnormalities	Supplemental Video 15 Supplemental Figure 17
CPVT2e	3	ISO (10 μM)	Regional conduction block caused by localized Ca^{2+} transient abnormalities	Supplemental Video 13

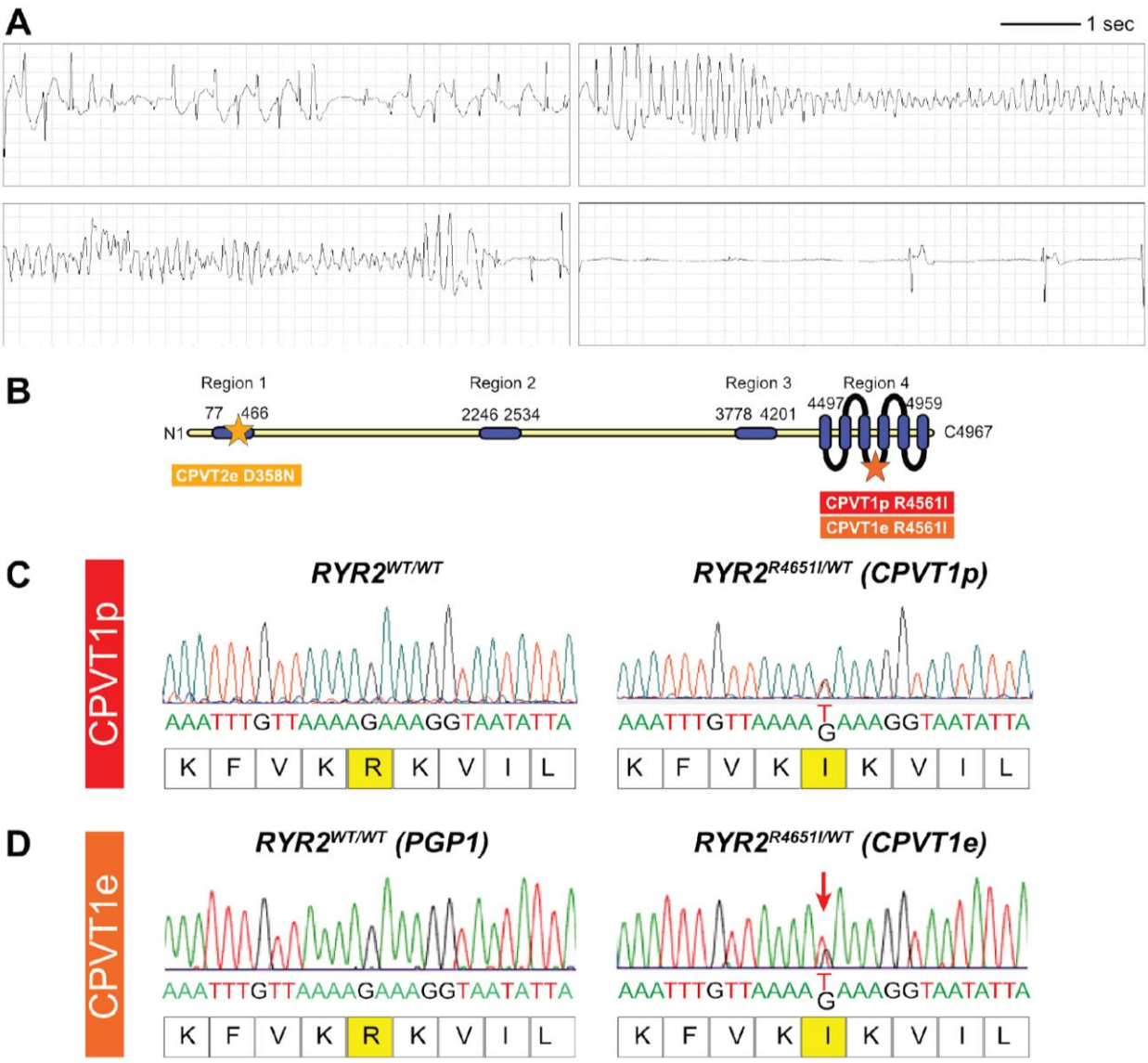

Supplemental Figure 1. iPSC lines with CPVT mutations in RYR2. A. Electrocardiography data from an implanted cardiac monitoring system. The patient developed bidirectional ventricular tachycardia (upper left), which converted into polymorphic ventricular tachycardia (upper right and lower left). The patient spontaneously recovered to a sinus rhythm (lower right). **B.** Schematic of RYR2 protein with mutation hotspot regions (Regions 1-4) and the location of the D358N and R4651I mutations within regions 1 and 4, respectively. **C.** Sanger sequencing of normal and patient-derived iPSCs (CPVT1p). Arrow indicates point mutation. **D.** Sanger sequencing of PGP1 wild-type iPSCs and isogenic, heterozygous RYR2 mutations at positions 4651 (CPVT1e), introduced by Cas9 genome editing. Arrow indicates point mutation.

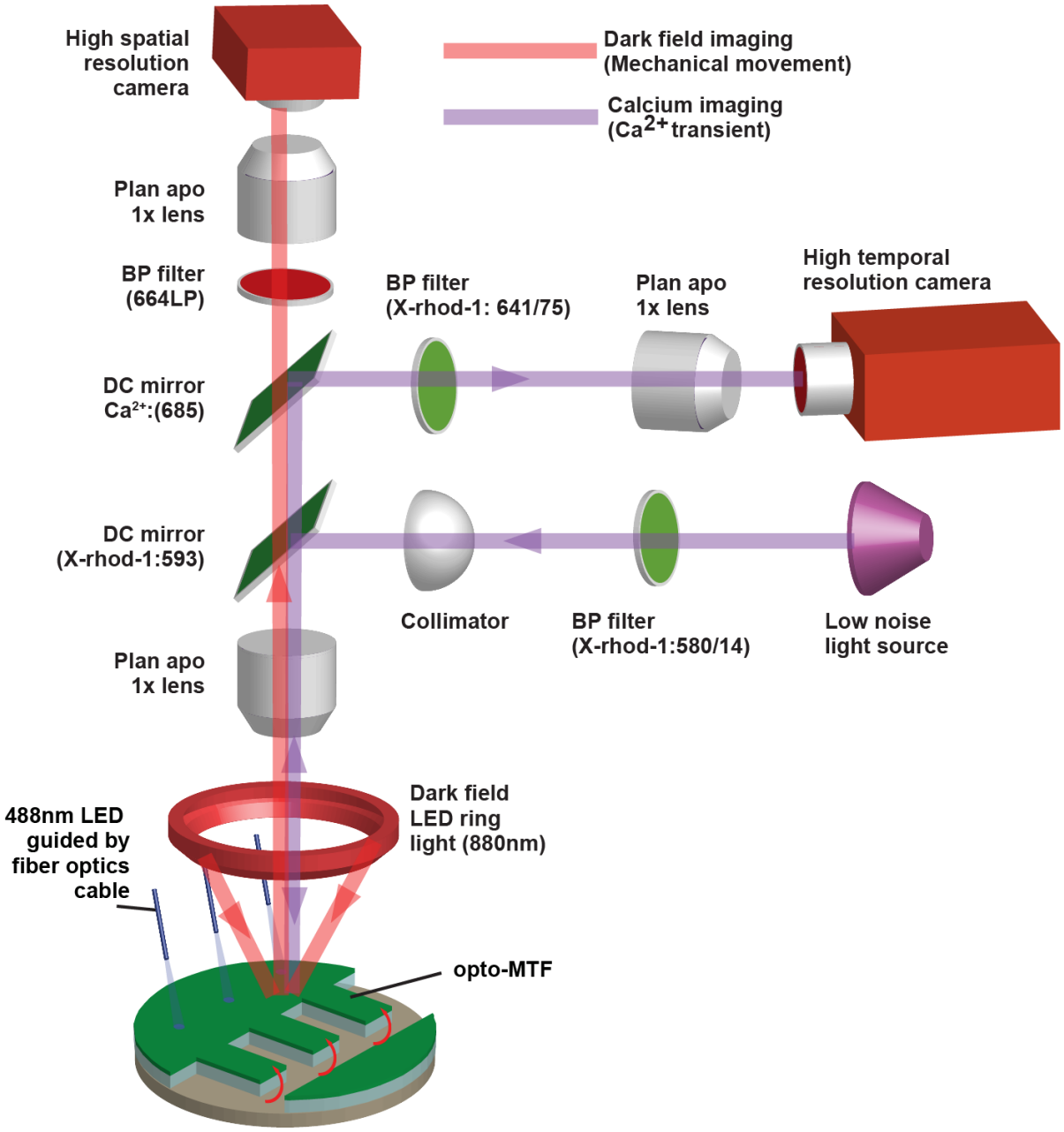

Supplemental Figure 2. Opto-MTF recording platform. Optical fibers stimulate focal areas on opto-MTF. Opto-MTF is illuminated under a microscope for simultaneous dark field imaging of mechanical cantilevers using a high spatial resolution camera, and fluorescent imaging of Ca^{2+} wave propagation using a high sensitivity, high speed camera.

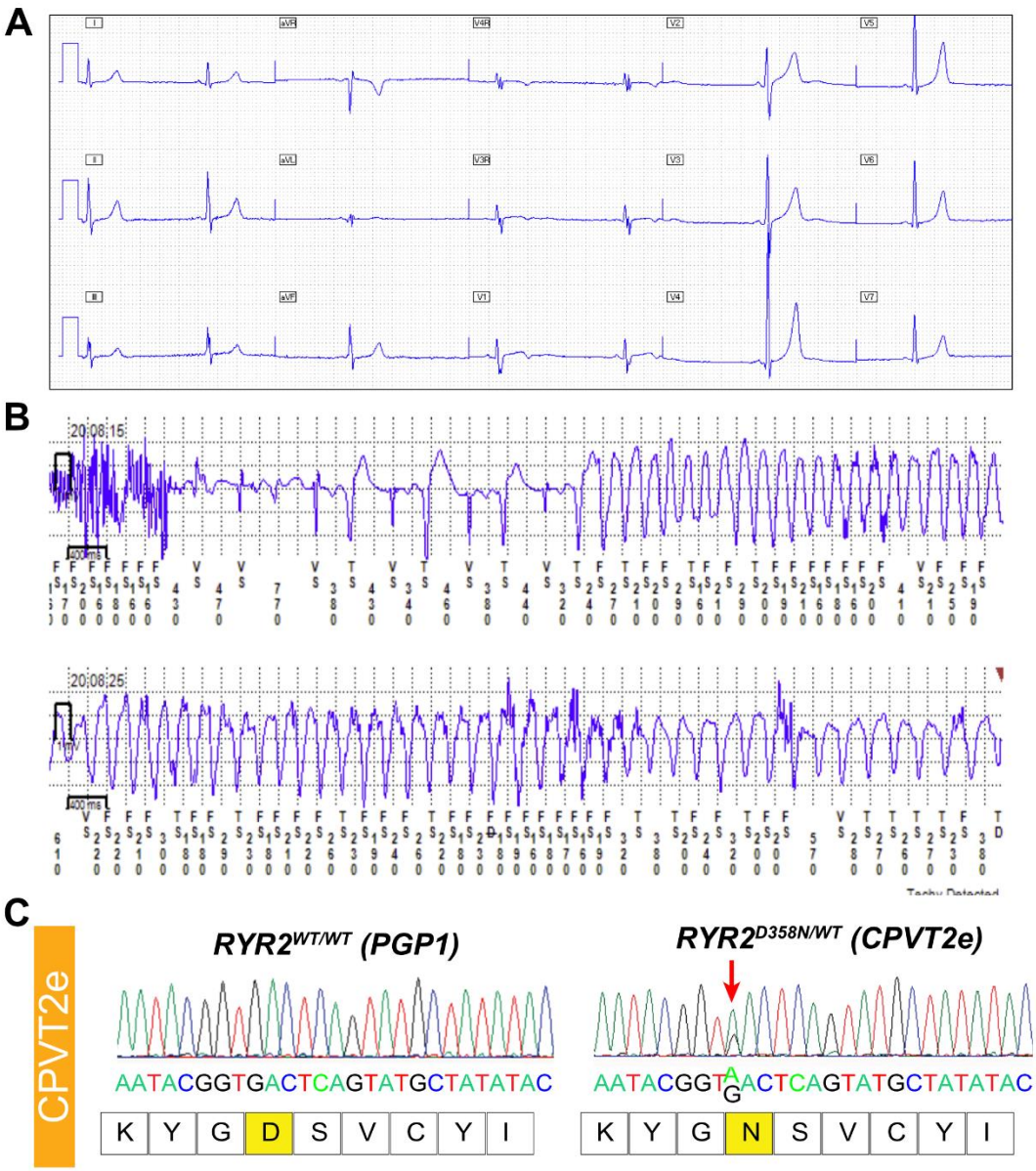

Supplemental Figure 3. Engineering a CPVT iPSC line by introducing a patient-derived RYR2-D358N mutation into wild-type PGP1 iPSCs. A. Baseline EKG from CPVT patient with RYR2-D358N mutation demonstrating sinus bradycardia. **B.** Implantable loop recorder from same patient demonstrating initiation of ventricular tachycardia during exercise. **C.** Sequencing of PGP1 iPSCs before (left) and after (right, CPVT2e) Cas9 genome editing. The arrow indicates the Cas9-induced point mutation, which causes substitution of asparagine for aspartate at position 358.

S2808 SITE ON-TARGET SEQUENCES IN WT, WT -S2802A, CPVT1e-S2808A																							SEQUENCING RESULTS		
chr1:+237660925	gRNA-RYR2	C	G	T	A	T	T	T	C	T	C	A	G	A	C	A	A	G	C	C	A	G	G		
S2808 SITE OFF-TARGET SEQUENCES IN WT, WT -S2802A, CPVTe -S2808A																							WT	WT-S2808A	CPVT1e S2808A
chr10:-17277114	VIM	G	T	·	·	·	·	·	·	·	·	·	·	A	·	·	A	·	·	C	A	·	√	√	√
chr11:+65657828	CCDC85B	·	T	·	G	·	·	·	·	·	·	·	·	A	G	·	·	·	·	G	A	·	√	√	√
chr19:-2429908	LMNB2	·	A	·	G	·	·	·	·	·	·	·	·	·	·	G	·	·	·	·	A	·	√	√	√
chr2:+215891569	ABCA12	·	A	C	·	·	·	·	·	·	·	C	·	·	·	T	·	·	·	·	A	·	√	√	√
chr3:+48450643	PLXNB1	T	·	A	·	G	·	·	·	·	·	·	·	A	·	·	·	·	·	T	·	·	√	√	√
chr4:+156654053	GUCY1A3	·	A	·	·	·	·	·	·	·	·	·	G	·	·	·	·	·	A	C	A	·	√	√	√
chr5:-171517221	STK10	G	A	G	·	·	·	·	·	·	·	·	G	·	·	·	·	·	·	T	·	·	√	√	√
chr7:-92158738	RBM48	·	·	·	·	·	·	·	·	G	·	·	A	·	T	·	·	·	·	T	A	·	√	√	√
chr9:+117407893	C9orf91	·	·	·	·	·	·	·	·	·	·	·	·	T	·	·	G	T	·	·	T	A	·	√	√	√

S2814A SITE ON-TARGET SEQUENCES IN WT, WT -S2814A, CPVT1e-S2814A																							SEQUENCING RESULTS		
chr1:+237666498	gRNA-RYR2	C	A	A	A	T	G	A	T	C	T	A	G	G	T	T	T	C	T	G	T	G	G		
S2814A SITE OFF-TARGET SEQUENCES IN WT, WT -S2814A, CPVTe -S2814A																							WT	WT-S2814A	CPVT1e S2814A
chr1:-47737803	STIL	·	·	·	·	·	·	G	A	G	·	T	·	·	·	·	·	·	·	·	·	·	·	√	√	√
chr1:+115113353	BCAS2	·	·	T	·	·	·	·	A	·	·	·	·	A	·	·	·	·	·	·	A	A	·	√	√	√
chr1:-202863852	KLHL12	G	·	T	·	·	·	·	·	·	·	·	T	·	·	C	·	·	·	·	G	A	·	√	√	√
chr1:-244166694	LOC339529	G	·	G	·	·	·	·	·	·	C	·	·	·	C	·	·	·	·	·	·	·	·	√	√	√
chr11:+32781831	CCDC73	A	·	·	·	·	T	·	·	·	·	·	·	·	·	·	·	T	·	C	A	A	·	√	√	√
chr11:+101857538	KIAA1377	T	·	·	C	·	·	·	·	G	·	·	A	·	·	·	·	·	·	·	·	A	C	√	√	√
chr12:+6797397	ZNF384	·	·	·	·	·	T	G	·	·	·	·	·	·	·	·	A	·	A	·	G	·	·	√	√	√
chr12:105611346	APPL2	·	·	·	·	·	A	·	·	T	·	·	·	·	·	C	·	·	·	A	A	·	·	√	√	√
chr12:+133281120	PXMP2	·	·	·	·	·	·	·	A	·	·	G	·	·	·	G	A	·	·	·	A	·	·	√	√	√
chr13:-115089778	CHAMP1	·	·	·	C	A	·	·	G	·	C	·	·	·	·	·	·	·	·	·	A	·	·	√	√	√

D358N SITE ON-TARGET SEQUENCES IN WT, CPVT2e																							SEQUENCING RESULTS	
chr1：+237441360	gRNA-RYR2	G	G	A	A	C	A	T	C	T	G	A	A	A	T	A	A	A	A	T	A	C	G	
D358N SITE OFF-TARGET SEQUENCES IN WT, CPVT2e																							WT	CPVT2e
chr1：-47142995	EFCAB14	·	A	·	·	·	·	·	·	·	·	·	·	·	·	·	·	T	·	·	T	·	A	√	√
chr1：-157801294	CD5L	·	·	·	·	·	·	·	T	·	·	·	·	·	·	·	·	·	·	·	G	T	·	√	√
chr1：+160589534	SLAMF1	·	·	T	T	·	·	·	·	·	C	·	·	·	·	·	·	·	·	·	·	T	A	√	√
chr1：-169551867	F5	T	·	G	·	·	T	·	·	·	·	·	·	·	·	·	C	·	·	·	·	A	A	√	√
chr1：+225446883	DNAH14	·	·	·	G	·	·	·	T	·	·	·	C	·	·	·	·	·	·	·	C	·	T	·	√	√
chr11：-46868085	LRP4-AS1	T	·	·	·	·	·	·	·	·	·	·	·	·	·	T	·	·	·	·	·	A	A	√	√
chr12：+19444669	PLEKHA5	A	·	·	·	·	T	·	·	·	T	·	·	·	·	·	T	·	·	·	·	·	A	√	√
chr12：+70932821	PTPRB	·	·	·	G	A	·	·	A	·	·	·	·	·	·	·	G	·	·	·	·	A	A	√	√
chr13：+25672335	PABPC3	·	C	·	·	A	·	·	·	·	A	·	·	·	·	·	·	·	·	A	·	T	·	√	√
chr2：+152108170	RBM43	T	·	·	·	G	·	·	·	·	·	·	·	·	·	T	·	·	·	A	·	·	A	√	√

R4651I SITE ON-TARGET SEQUENCES IN WT, CPVT1e, CPVTe -S2808A, CPVT1e-S2814A																								SEQUENCING RESULTS			
chr1:+237795309	gRNA-RYR2	G	A	C	A	A	A	T	T	T	G	T	T	A	A	A	A	G	A	A	A	G	G				
R4651I SITE OFF-TARGET SEQUENCES IN WT, CPVT1e, CPVTe -S2808A, CPVTe-S2814A																								WT	CPVT1e	CPVT1e S2808A	CPVT1e S2814A
chr1:+100606645	TRMT13	·	·	A	·	C	·	·	·	·	C	·	·	·	·	·	·	·	·	·	·	·	·	√	√	√	√
chr1:+180399426	ACBD6	·	·	·	·	·	·	·	G	G	·	·	·	·	·	·	·	C	·	·	T	·	·	√	√	√	√
chr10:+30992505	SVILP1	·	·	·	G	·	T	·	·	·	·	·	·	C	·	·	·	·	·	·	·	·	·	√	√	√	√
chr10:+97916968	ZNF518A	·	·	·	·	·	·	·	A	·	·	A	A	·	·	·	·	·	·	·	T	G	·	√	√	√	√
chr10:+124749930	PSTK	T	·	·	·	·	·	·	·	·	·	·	·	·	·	·	·	C	·	·	C	G	·	√	√	√	√
chr14:-58926797	KIAA0586	A	·	·	·	·	T	·	A	·	·	·	·	·	·	·	·	·	·	·	C	·	·	√	√	√	√
chr15:+34145265	RYR3	·	·	·	·	·	G	·	·	·	·	·	A	·	·	G	·	·	·	·	·	G	·	√	√	√	√
chr15:+96880950	NR2F2	T	·	·	·	·	G	·	·	·	·	C	·	·	·	·	·	·	·	·	G	·	·	√	√	√	√
chr18:+14799398	ANKRD30B	·	G	A	·	·	·	·	·	·	·	A	·	·	·	·	·	T	·	·	T	G	·	√	√	√	√
chr2:+168098324	XIRP2	·	·	·	T	·	·	G	·	·	·	·	·	·	·	·	·	·	·	G	C	·	·	√	√	√	√

Supplemental Figure 4. Summary of Sanger sequencing of the top predicted off-target sites for each guide RNA. The top 10 off target sites for each guide RNA used for genome editing were computational predicted (see Methods). Amplicons containing these regions were amplified from the genomic DNA of iPSC lines exposed to Cas9 and the guide RNA. We did not detect mutations at these predicted off-target sites.

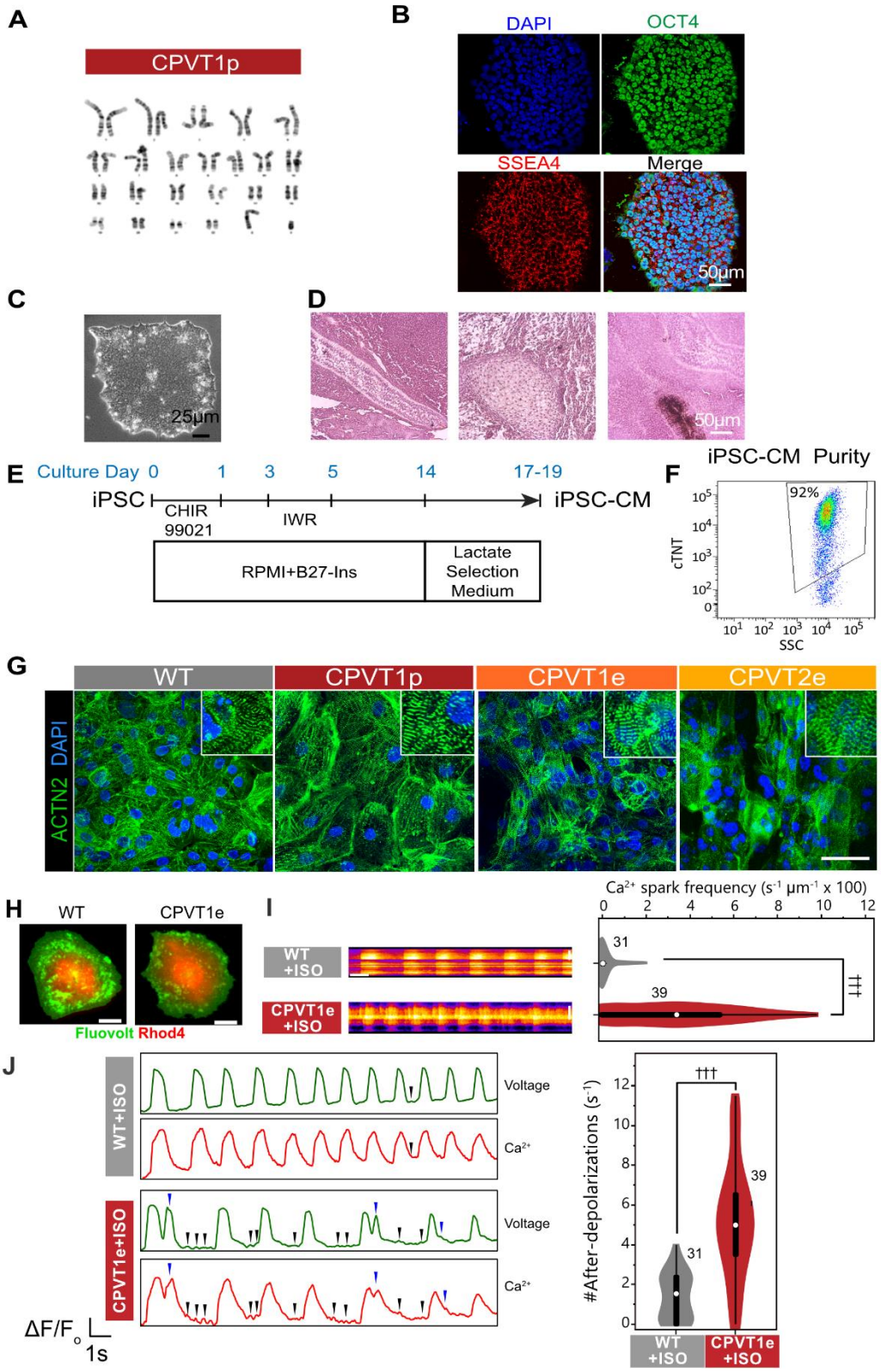

Supplemental Figure 5. Characterization and genome editing of CPVT iPSC lines. A–D. Quality control of CPVTp iPSC line. CPVTp cells had normal karyotype (**A**), expression of pluripotency markers (**B**), typical colony morphology (**C**), and formed teratomas that produced derivatives from three germ layers, as assessed by H&E staining of histological sections (**D**). **E.** Protocol used to differentiate

iPSC-CMs from iPSCs. **F.** FACS plot showing purity of lactate-selected iPSC-CMs. **G.** iPSC-CM sheets grown isotropically on unpatterned gelatin. The iPSC-CMs were highly pure and formed sarcomere structures. Insets show magnified views. **H-J.** Simultaneous recording of intracellular Ca^{2+} and membrane voltage of single, isolated iPSC-CMs using Rhod4 and Fluovolt, respectively. H, confocal images of dye-loaded iPSC-CMs. Bar, 10 µm. I, Ca^{2+} sparks in single, isolated iPSC-CMs treated with ISO, measured by confocal line scan imaging. Left panel, representative confocal line scan imaging. Horizontal bar, 1 sec. Vertical bar, 20 µm. Right panel, quantification. J, Simultaneous recording of Ca^{2+} and membrane voltage from spontaneously beating, single iPSC-CMs treated with ISO by confocal line scan imaging. Left panel, representative traces. Early and late after-depolarizations are indicated by blue and black triangles, respectively. Right panel, quantification of the frequency of after-depolarizations per cell. Wilcoxon: †††, $P<0.001$. Numbers next to violin shapes indicate sample size.

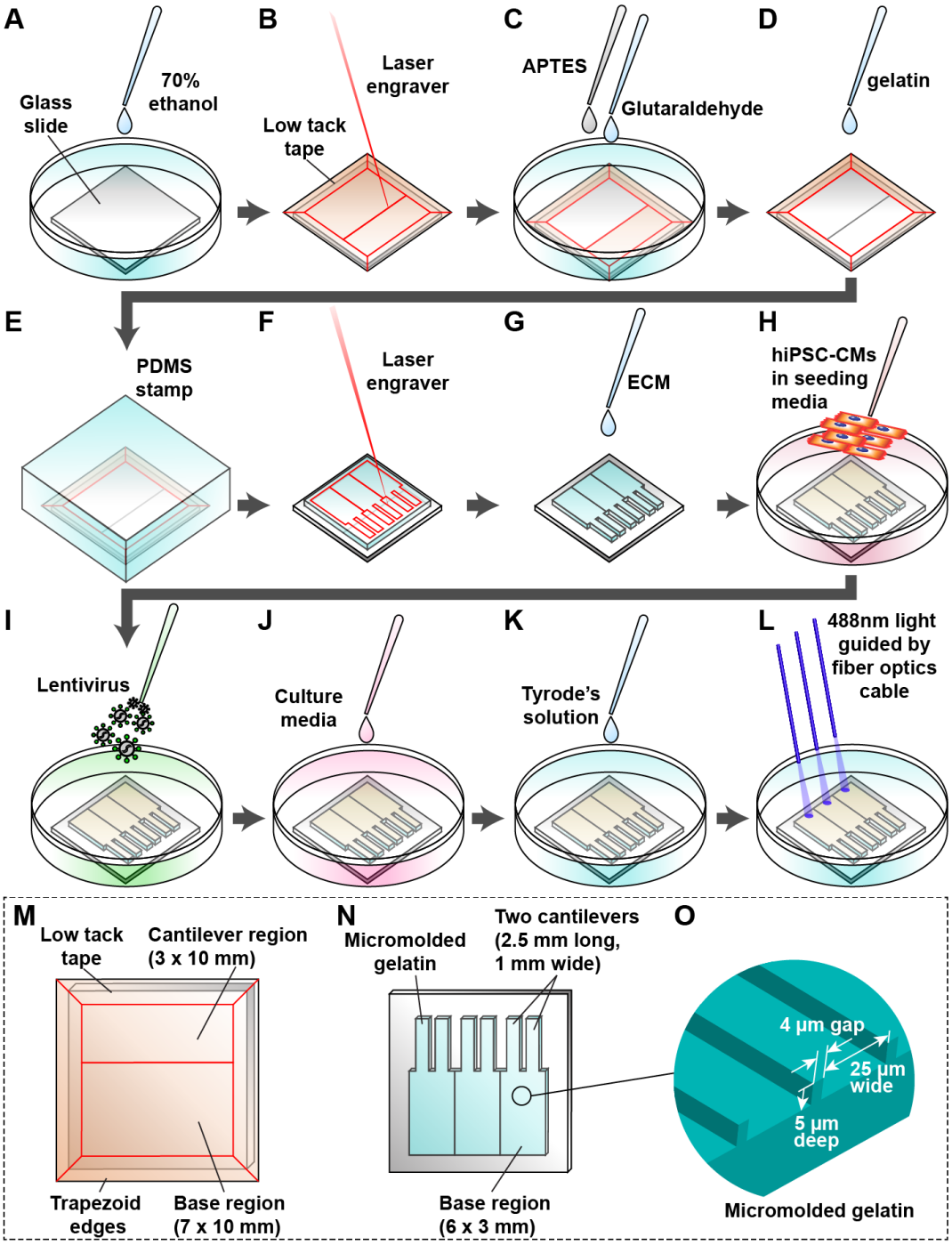

Supplemental Figure 6. Fabrication of opto-MTFs seeded with hiPSC-CMs. A. Glass coverslip was cleaned using ethanol. **B.** After the coverslip was covered with low-adhesive tape, the tape was laser cut to have two inner rectangles, which are for cantilever and base region of the opto-MTF. **C.** After peeling off only the base region tape, the coverslip was activated with APTES and glutaraldehyde. **D.** After peeling off the cantilever region tape, the gelatin and MTG mixture were pipetted onto the coverslip. **E.** Gelatin was cured overnight while a PDMS stamp with micro-groove line pattern was applied. **F.** The micromolded gelatin was laser cut to form the outline of opto-MTF. **G.** Gelatin chip was hydrated with ECM mixture. **H.** Opto-MTF was seeded with hiPSC-CMs to form engineered tissues. **I.** After 2 days, the engineered opto-MTF tissues were transduced with ChR2 lentivirus. **J.** After 1 day, lentivirus-

containing medium was replaced with fresh culture medium. **K.** At post-transduction day 3, the opto-MTF cantilevers were gently peeled off in Tyrode's solution. **L.** While opto-MTF was optically stimulated, Ca^{2+} and dark field images were simultaneously acquired. **M–O.** Geometry and dimensions of engraved tape (**M**), gelatin opto-MTF (**N**), and micro-groove (**O**).

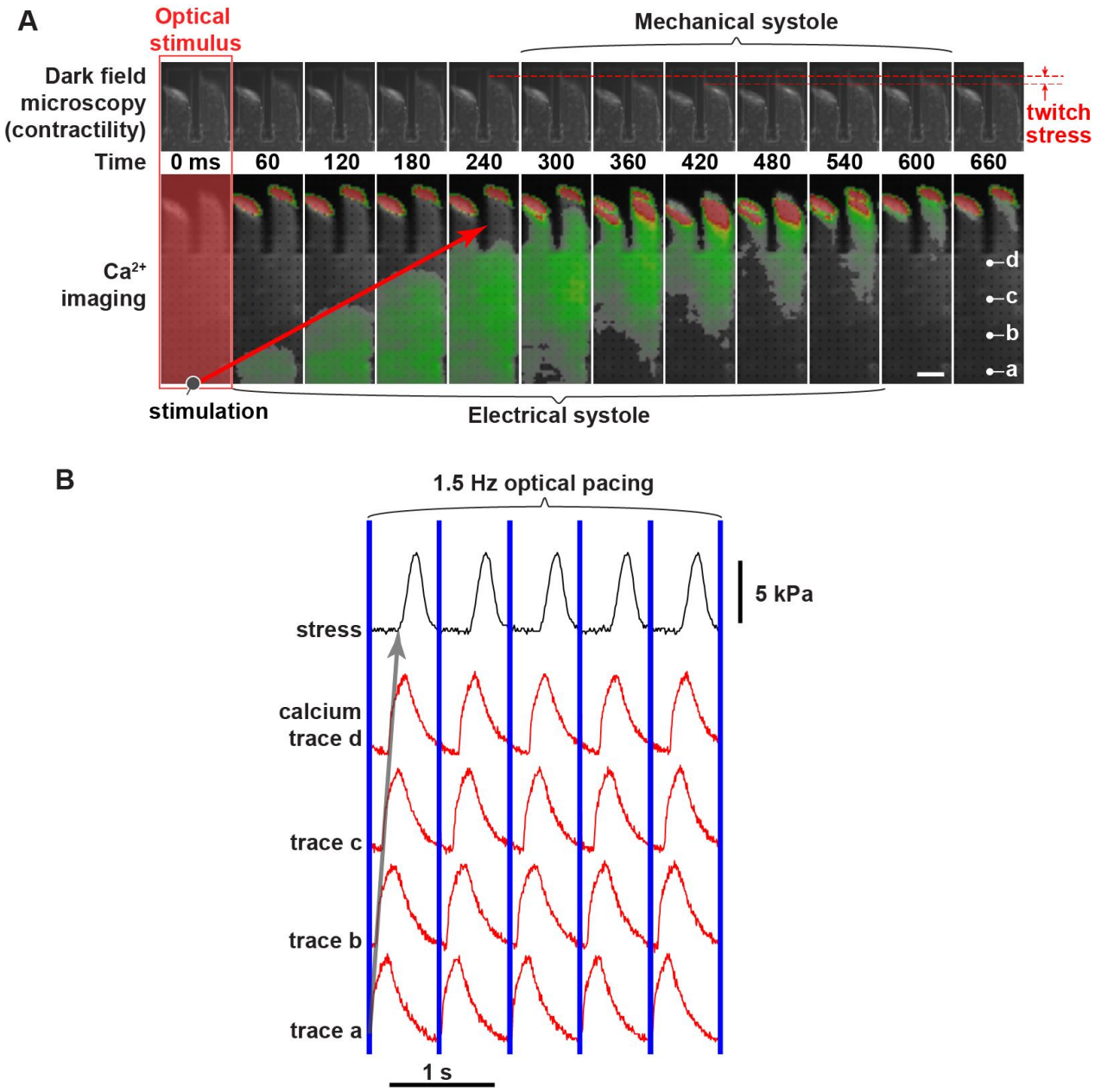

Supplemental Figure 7. Optical mapping of Ca^{2+} wave propagation in a WT opto-MTF. A. Time lapse images of opto-MTF showing X-Rhod-1 signal ("Ca^{2+} imaging") and dark field imaging of deformable cantilevers at the terminus of the MTF. Bar = 1 mm. **B.** Ca^{2+} transients and mechanical stress in MTFs. Ca^{2+} X-Rhod-1 signal was recorded at points a-d, labeled in the right-most image of (**A**). Blue lines indicate 488 nm optical pacing signals.

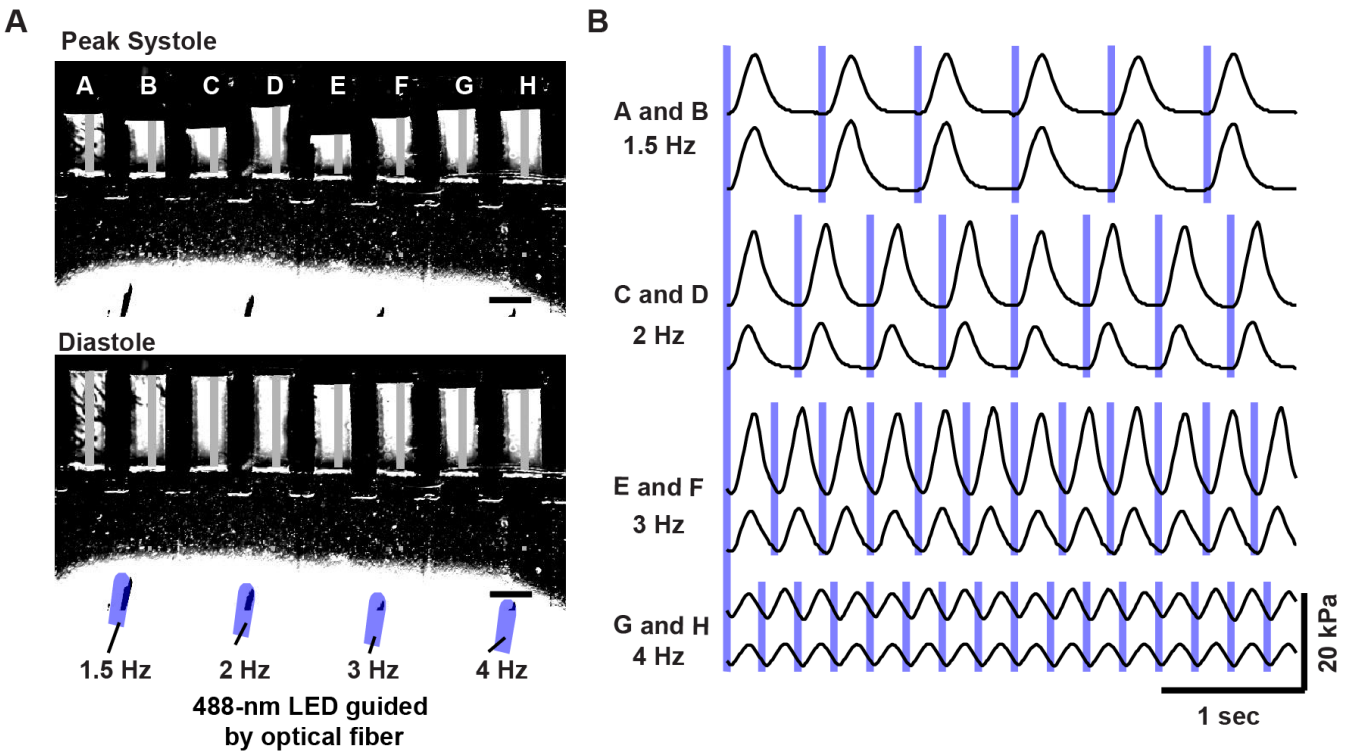

Supplemental Figure 8. Independence of adjacent MTFs in opto-MTF construct. A. Peak systolic and diastolic contraction of MTFs upon independent optical stimulation on NRVM opto-MTFs with different pacing frequencies (1.5, 2, 3, and 4 Hz). Bar = 1 mm. **B.** Stress traces of each MTF. Each MTF, connected to a pair of cantilevers, was stimulated by a separate optical fiber at a different frequency. The mechanical systole of each MTF's cantilever pair was independent of the other MTFs, as demonstrated here by the different frequencies of the stress traces. Blue lines indicate optical pacing.

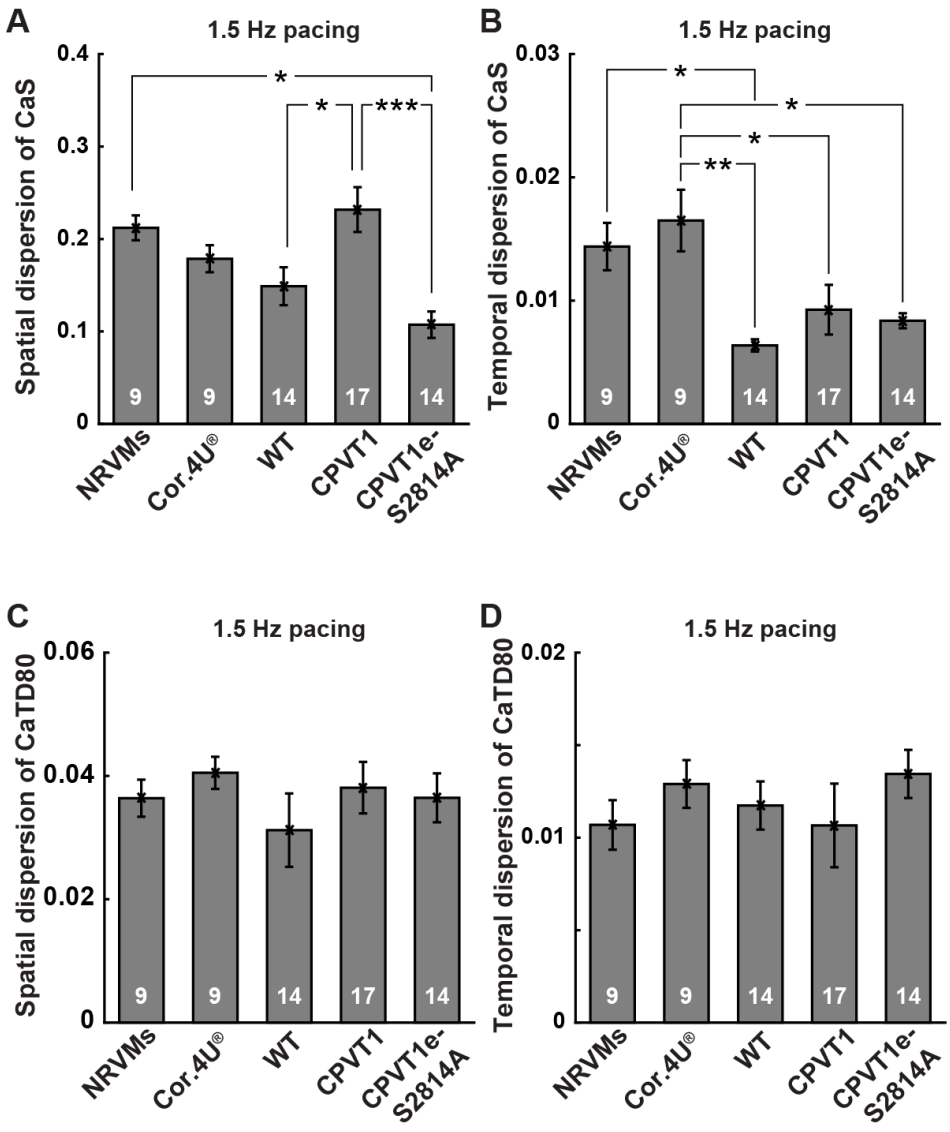

Supplemental Figure 9. Spatial and temporal dispersion of speed and calcium transient duration in opto-MTFs. A. Spatial dispersion of Ca^{2+} wave propagation speed (CaS). **B.** Temporal dispersion of CaS. **C.** Spatial dispersion of Ca^{2+} transient duration at 80% recovery (CaTD80). **D.** Temporal dispersion of CaTD80. Heterogeneities of CaS and CaTD80 were calculated for opto-MTFs constructed using the indicated cells: NRVMs, neonatal rat ventricular cardiomyocytes; Cor.4U, human stem cell-derived cardiomyocytes from Axiogenesis; WT, CPVT1 (pooled CPVT1e and CPVT1p), and CPVT1e-S2814A, iPSC-CMs from this study. Error bars represent SEM. Tukey-Kramer honestly significant difference pairwise test: *, P<0.05. **, P<0.01. ***, P<0.001.

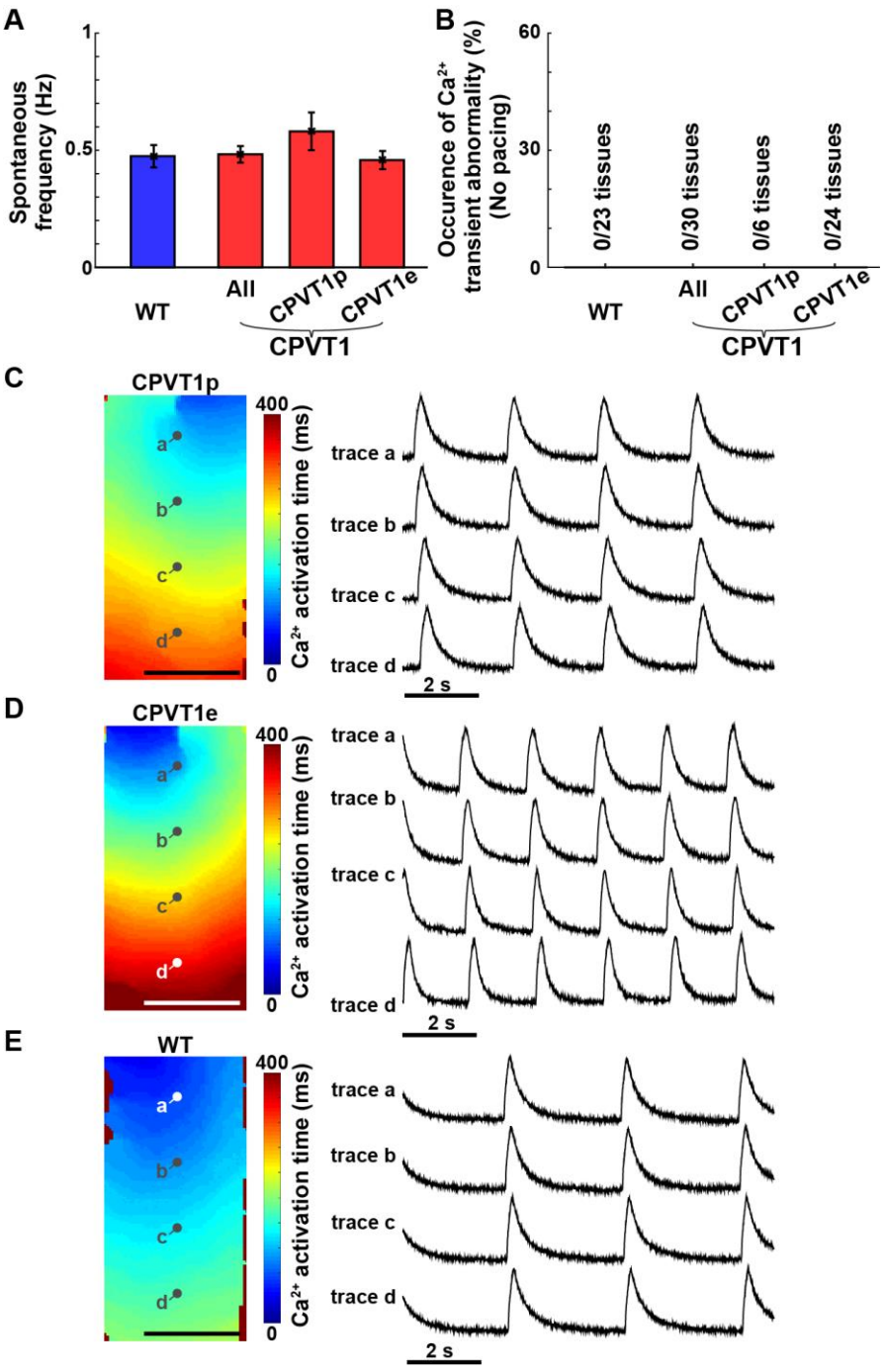

Supplemental Figure 10. Spontaneous Ca^{2+} waves in opto-MTFs. Opto-MTFs constructed from CPVT1p, CPVT1e, or WT iPSC-CMs allowed to beat spontaneously. Ca^{2+} waves were optically recorded by X-Rhod-1 fluorescence intensity. **A.** The spontaneous beating frequency of the opto-MTFs was comparable between iPSC-CM types. "All" represents the union of CPVT1p and CPVT1e tissues. Error bars represent SEM. **B.** Ca^{2+} tracings at individual pixels of the indicated tissues were analyzed for tissue-level Ca^{2+} transient abnormalities. None were observed in any of the spontaneously beating opto-MTFs. **C–E.** Ca^{2+} activation maps (left) and Ca^{2+} signal traces (right) at indicated points on the opto-MTF. Note lack of aberrant Ca^{2+} transients. Spontaneous Ca^{2+} waves originated from the edges of the MTFs. Bar, 2 mm.

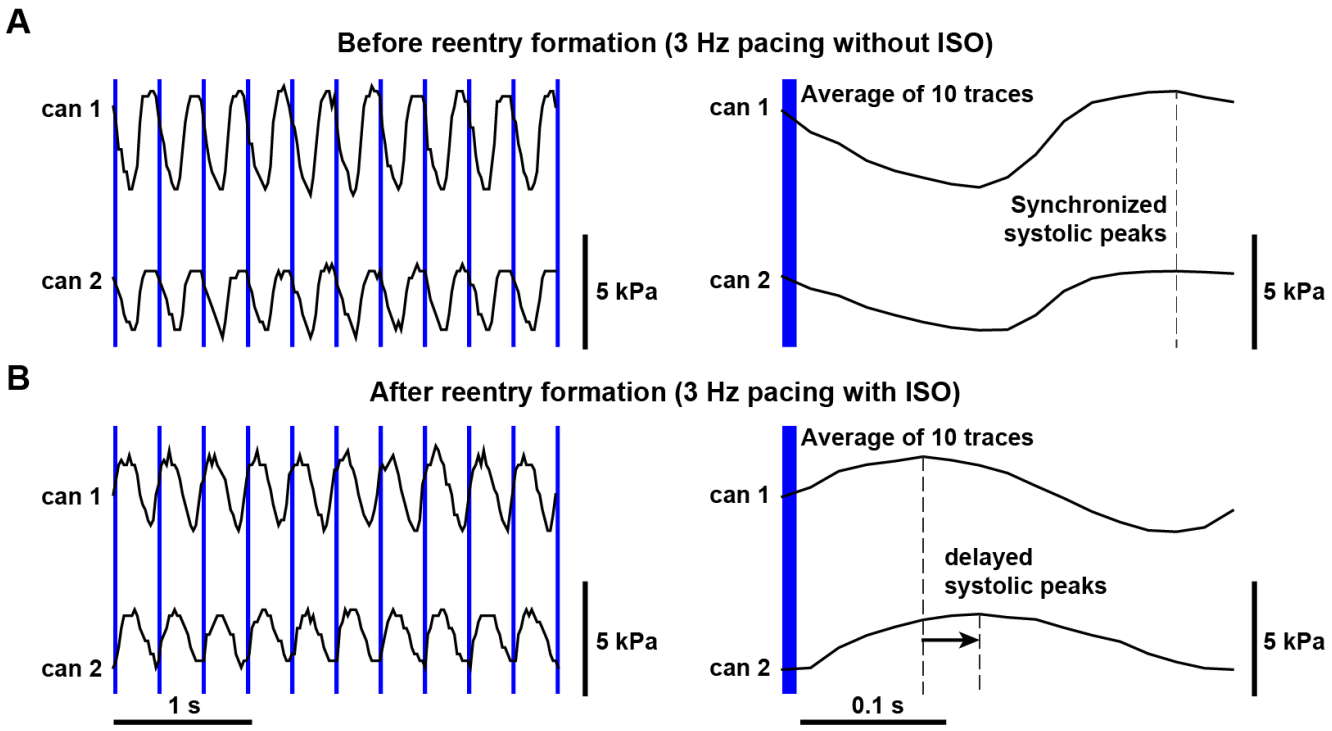

Supplemental Figure 11. Reentry in CPVT1p opto-MTFs. Asynchronous contraction of iPSC-CMs in opto-MTF cantilevers during reentry. **A.** With 1:1 capture (3 Hz pacing without ISO), the two cantilevers of a CPVT1p opto-MTF exhibited synchronized stress waveforms. **B.** During reentry (3 Hz pacing with ISO), the stress waveforms of the same opto-MTF became asynchronous. Time scale is expanded in traces on the right.

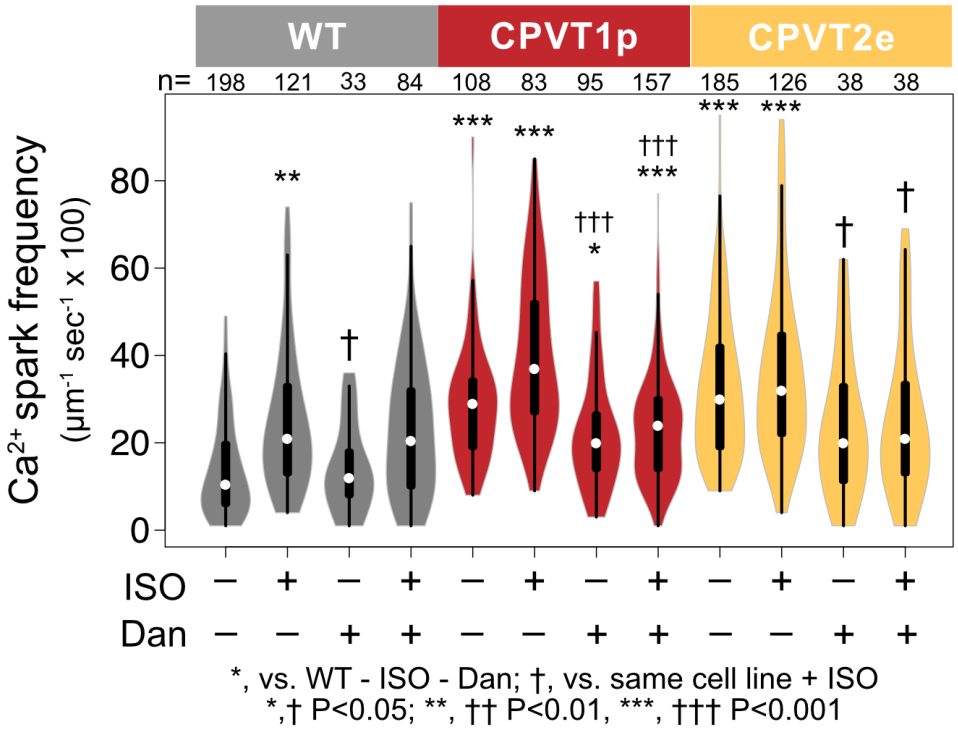

Supplemental Figure 12. Response of control and CPVT iPSC-CMs to dantrolene. Ca^{2+} spark frequency was measured by confocal line scan imaging of Fluo-4-loaded iPSC-CMs treated with isoproterenol (ISO) or dantrolene (Dan), as indicated. Steel-Dwass non-parametric test with multiple testing correction: *, compared to WT without ISO or dantrolene; †, compared to same line with ISO. *, † P<0.05; ** P<0.01; ***, ††† P<0.001

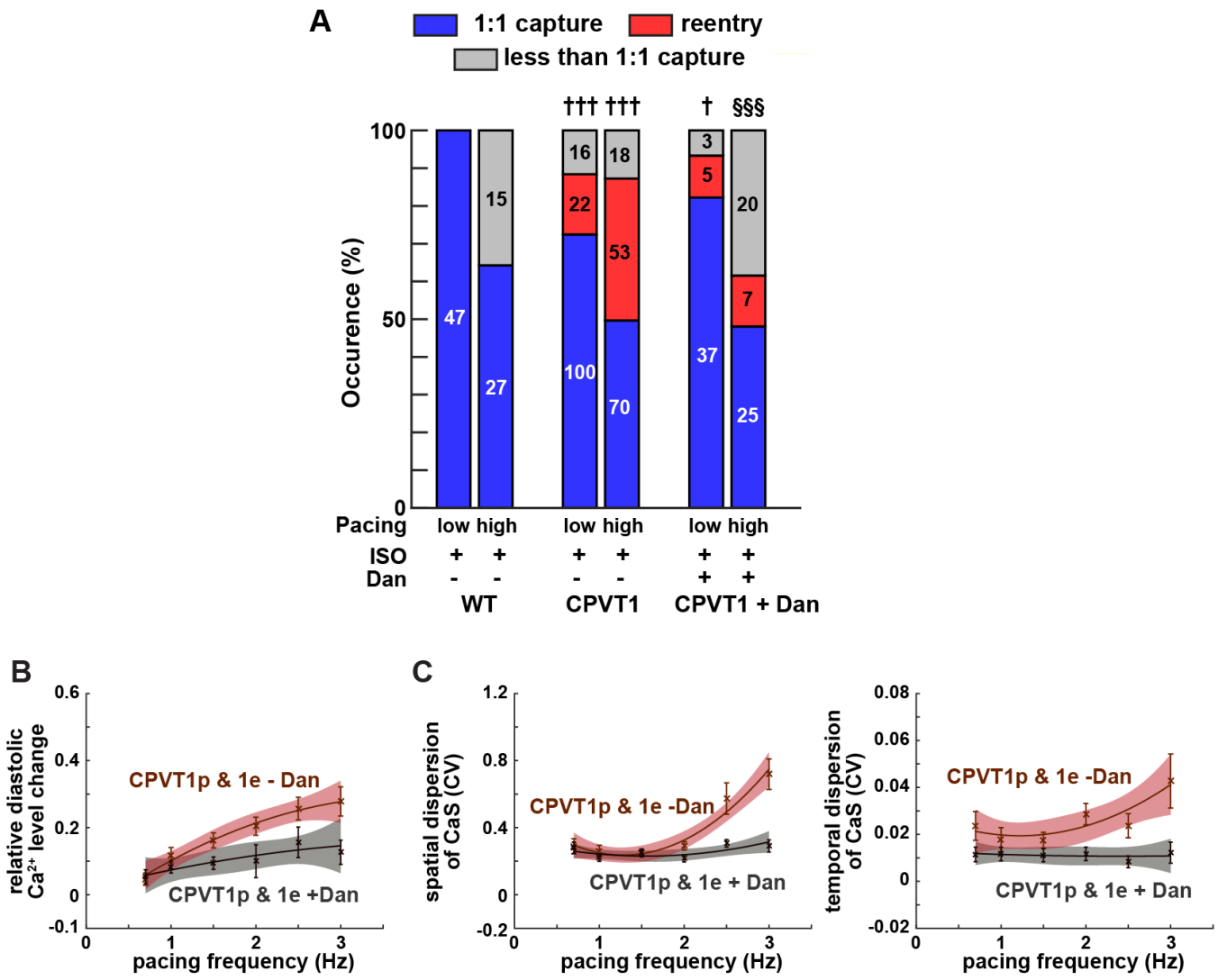

Supplemental Figure 13. Effect of dantrolene on CPVT1 tissue properties. A. Occurrence of reentry in CPVT1 (union of CPVT1p and CPVT1e) treated with dantrolene (Dan), compared to WT (†, †††) and CPVT1 without Dan (§§§) opto-MTFs under the matching conditions. Pearson's chi-squared test with Bonferroni correction for three possible pairwise comparisons: †, P<0.05/3. ††† or §§§, P<0.001/3. Bars are labeled with samples sizes. **B–C.** Relative diastolic Ca^{2+} level change from basal condition (**B**), and spatial and temporal dispersion of Ca^{2+} wave propagation speed (**C**) as a function of pacing frequency under ISO stimulation in CPVT1 before and after a Dan loading. Data from tissues with 1:1 capture were included (n=12 WT, 33 CPVT1p, 13 CPVT1e, 21 CPVT1+Dan, from > 3 harvests). Smooth lines are quadratic functions fit to the data. Shaded areas and error bars represent the 95% confidence interval for the fit and SEM, respectively.

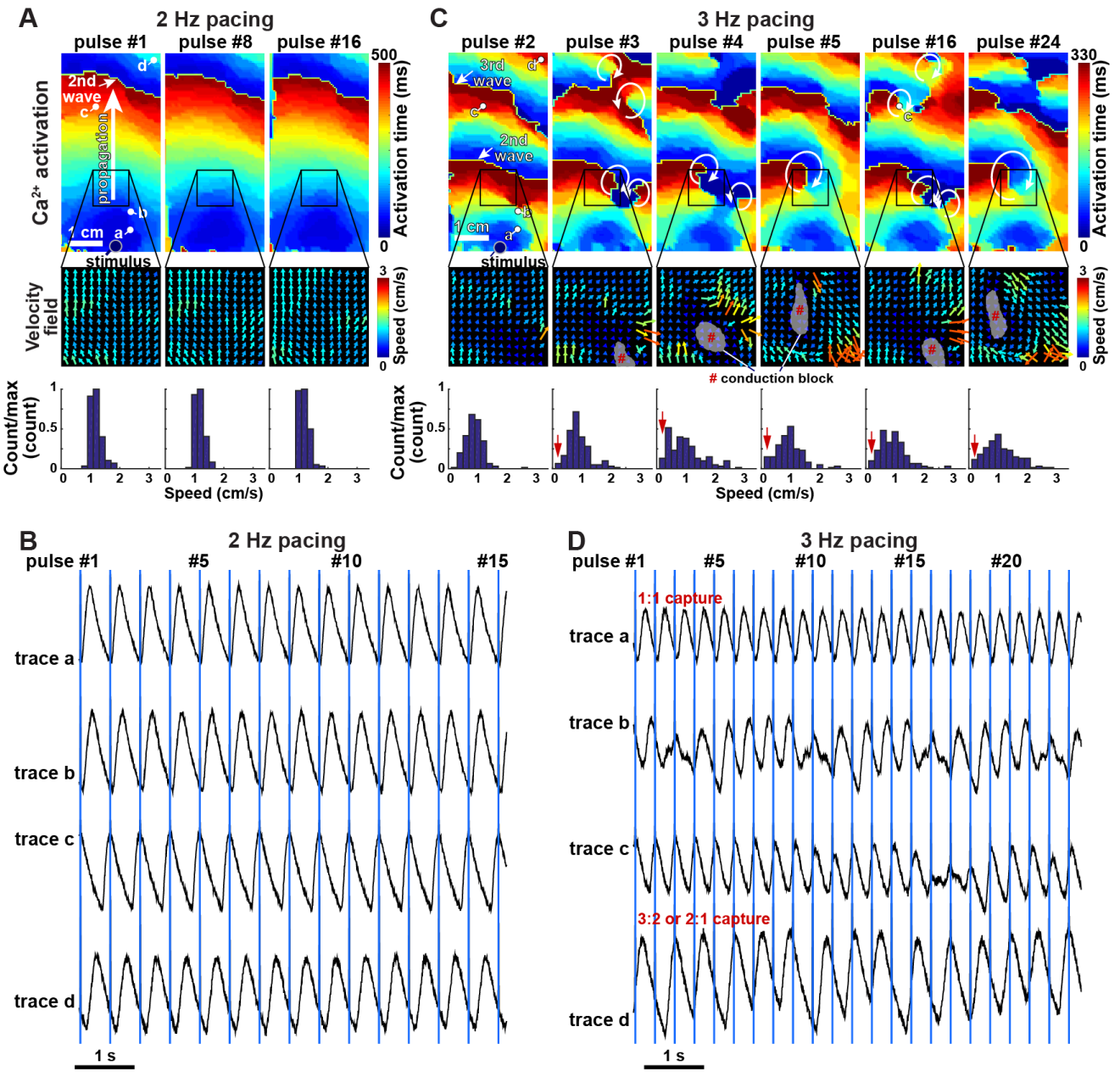

Supplemental Figure 14. Reentry in CPVT1e opto-MTF. A–B. Pacing at 2 Hz. Ca^{2+} waves are well-ordered. Ca^{2+} traces from points labeled in left panel of **A** are shown in **B**. **C–D.** Pacing of the same tissues at 3 Hz. Ca^{2+} waves are chaotic, and multiple areas of reentry from. Ca^{2+} traces from points labeled in left panels of **C** are shown in **D**. Note that the most distal point d has 3:2 or 2:1 coupling with the pacing stimulus. Activation maps and Ca^{2+} traces were calculated by processing Ca^{2+} imaging data in Supplemental Video 11 & 12.

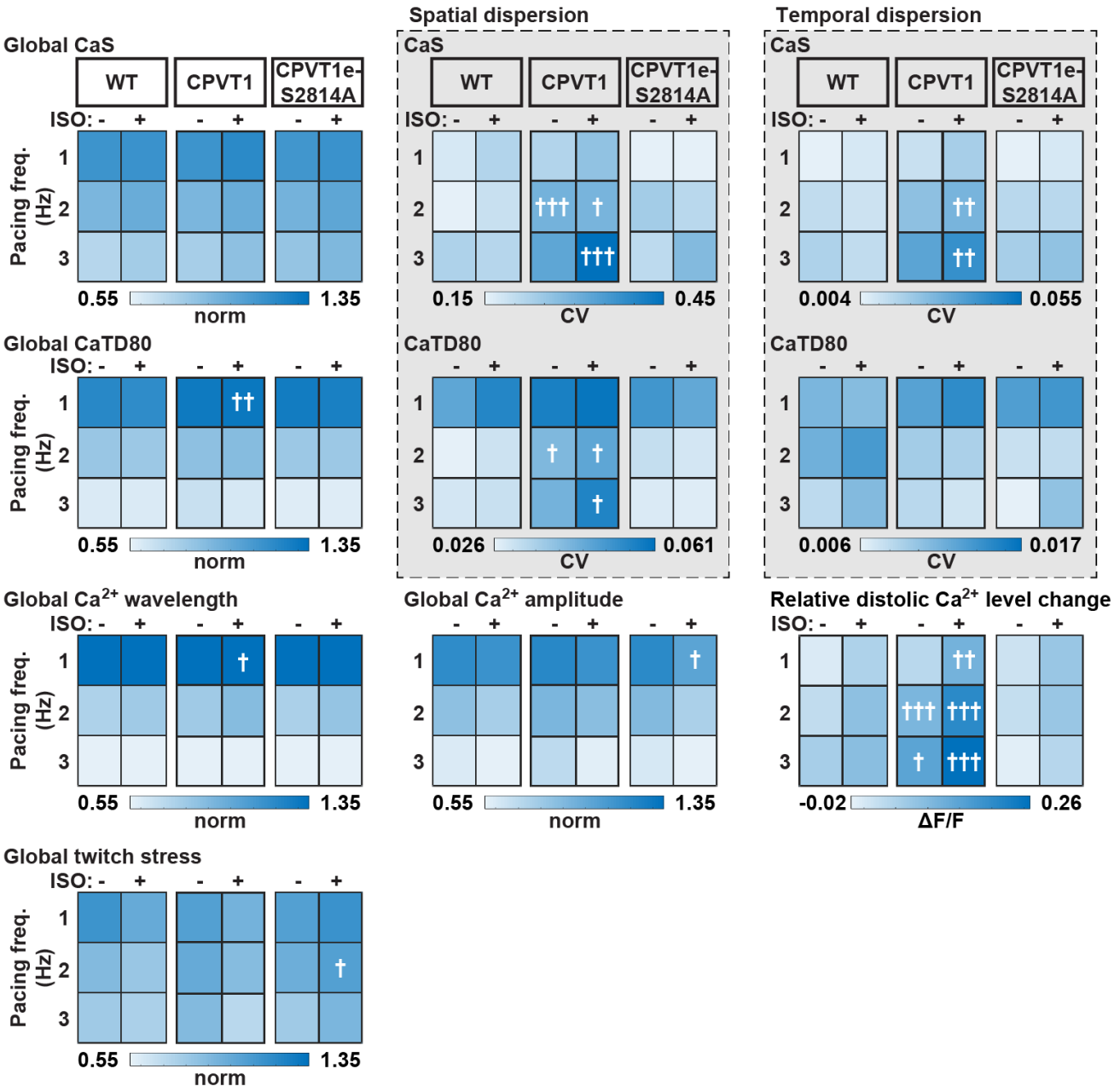

Supplemental Figure 15. Statistical analysis of opto-MTF properties. Parameters were analyzed with and without ISO treatment at 1, 2, and 3 Hz pacing frequencies. These 60 comparisons were made between WT and CPVT1 (union of CPVT1p and CPVT1e) and between WT and CPVT1e-S2814A under the matching conditions. The marks (†, P<0.05. ††, P<0.01. †††, P<0.001, student's t-test) indicates significant differences before Benjamini–Hochberg corrections for multiple comparisons (Fig. 3G and 6H). Data of global variables were normalized to values from the same opto-MTF at 1.5 Hz pacing without ISO. Only tissues responding 1:1 to every stimulus were included (n=12 WT, 33CPVT1p, 13 CPVT1e, and 18 CPVT1e-S2814A from > 3 harvests).

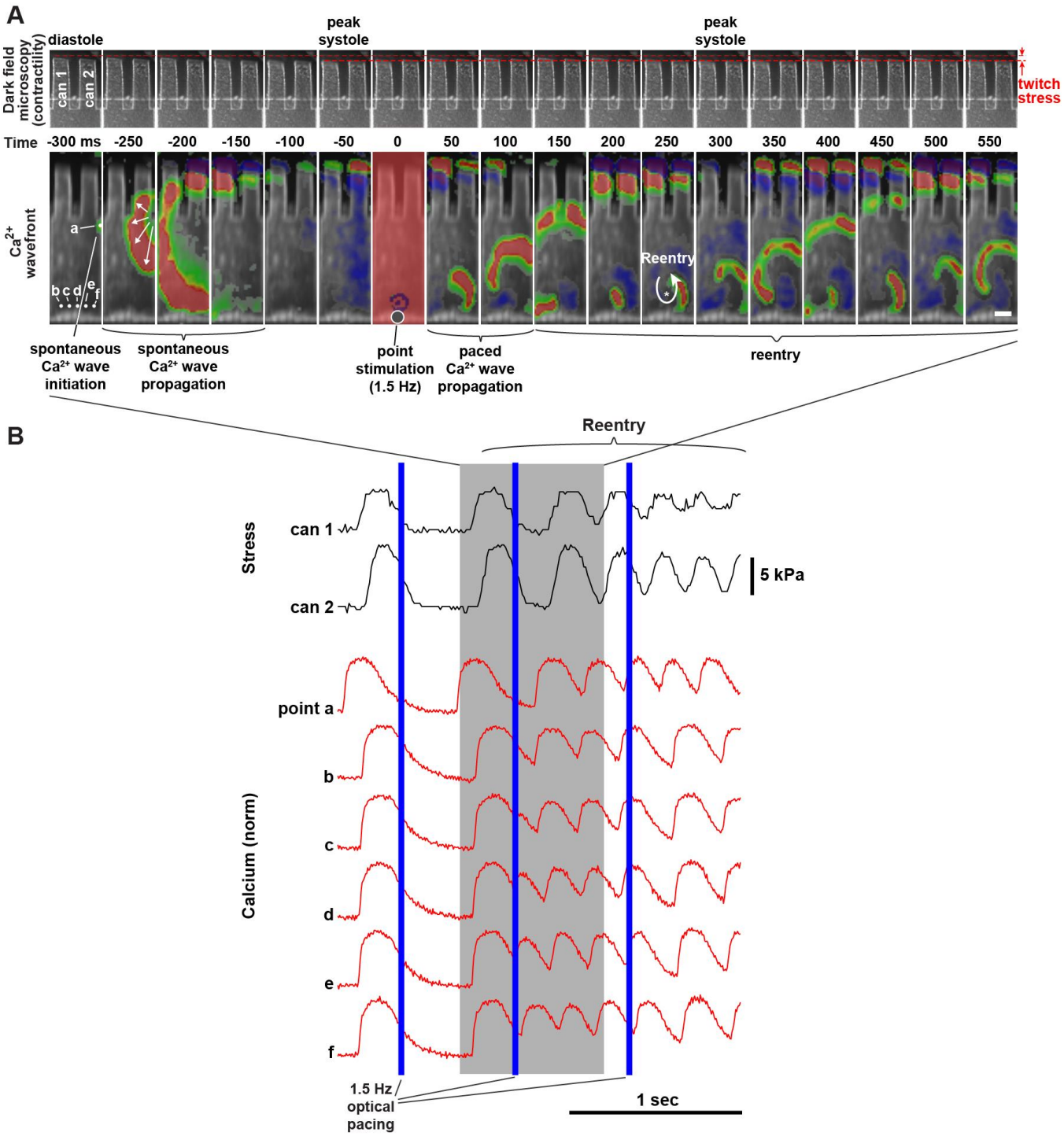

Supplemental Figure 16. Initiation of reentry during low pacing frequency by pacing during recovery from a spontaneous beat. a, Representative time lapse images show the wave front of a spontaneous Ca^{2+} wave originating from point a located on an edge of the tissue. Optical stimulation at 1.5 Hz at the labeled point initiated a paced Ca^{2+} wave as the local tissue recovered from the spontaneous wave, initiating reentry. Bar = 1 mm. **b,** Mechanical stress and Ca^{2+} traces recorded at the points labeled "can 1 and 2" and "a to f" in the left-most image of panel A. Blue lines indicate optical

pacing at the stimulation point. Pacing during the recovery phase of the spontaneous beat captured at point f but not point b. Images and traces were from Supplemental Video 10.

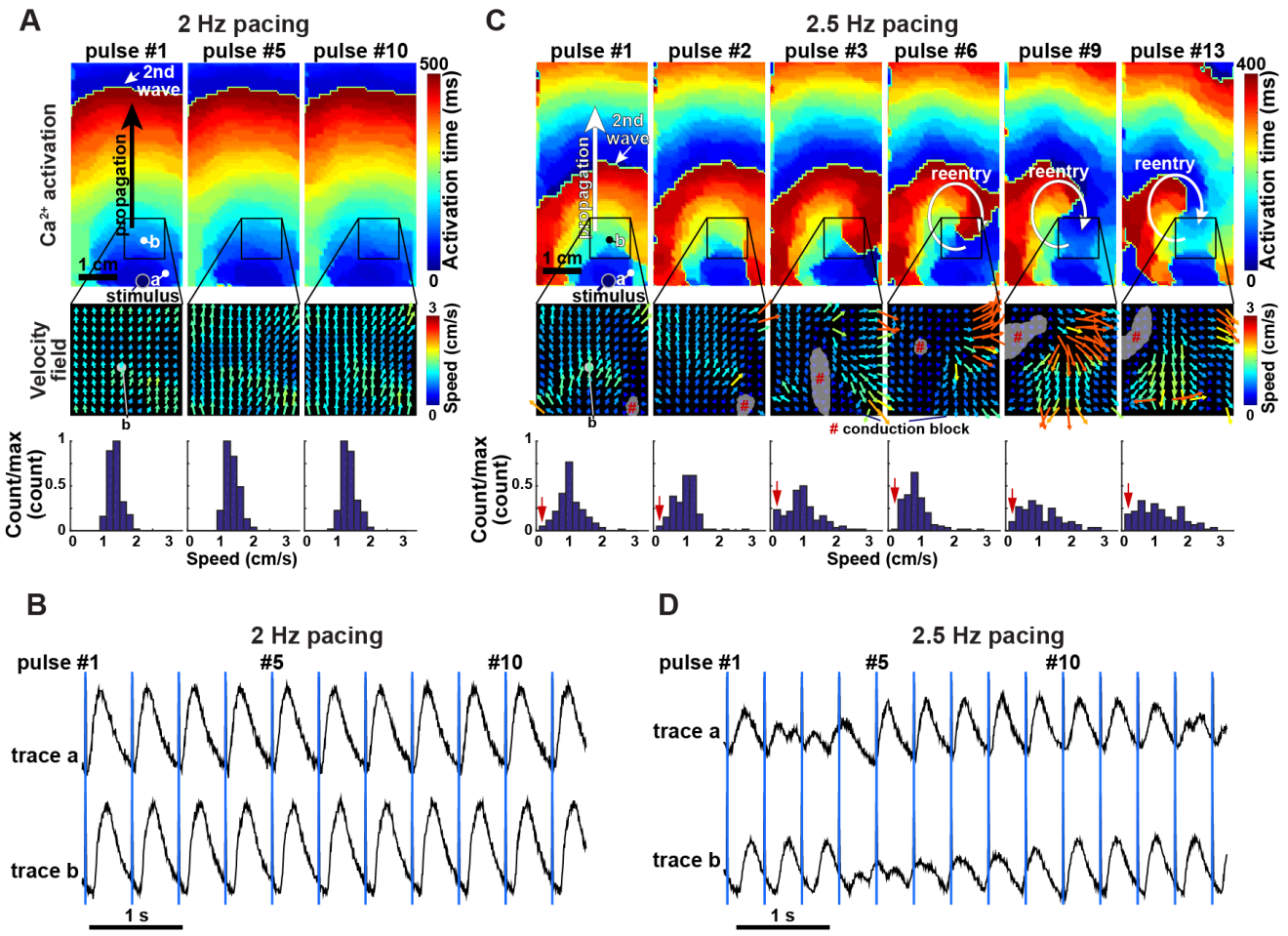

Supplemental Figure 17. Initiation of reentry in CPVT1e opto-MTF. A–B. Organized Ca^{2+} waves at 2 Hz pacing. Traces in **B** were recorded from points labeled in **A**. **C–D.** Development of reentry at 2.5 Hz pacing in the same tissue as **A** and **B**. Traces in **D** were recorded from points labeled in **C**. Reentry initiated around region of slow conduction and conduction block after pulse 2.

.

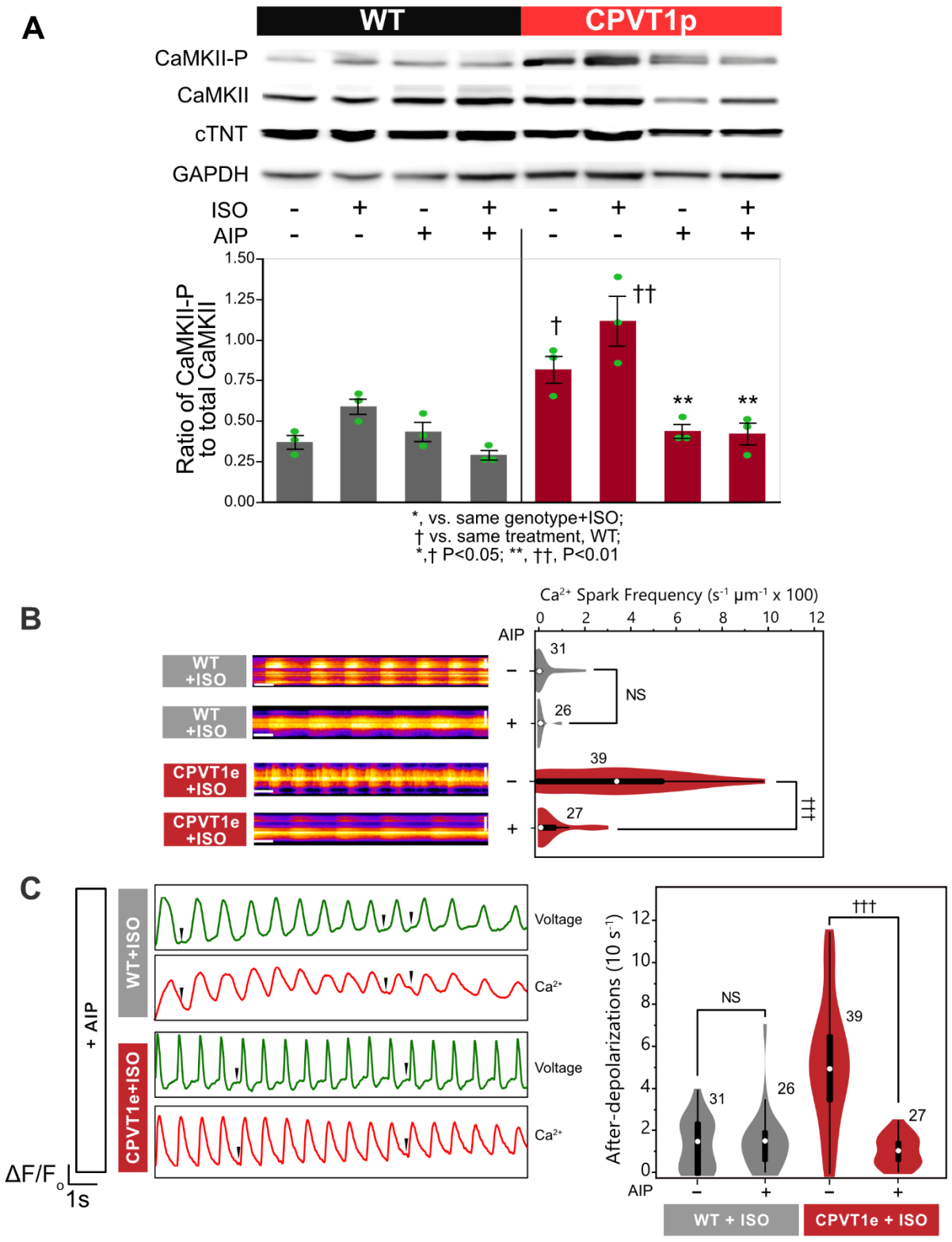

Supplemental Figure 18. Inhibition of CaMKII activity by cell permeable inhibitory peptide. A. iPSC-CMs were treated with the cell permeable CaMKII peptide inhibitor AIP (250 nM). Cells were stimulated for 60 minutes with 1 µM ISO prior to analyzing cell extracts by immunoblotting. In wild-type (PGP1) cells, CaMKII T286 phosphorylation was blocked by AIP. In CPVT1p cells, there was basal activation of CaMKII. This was blocked by AIP. Western blots show ratio of CaMKII-T286p

signal to total CaMKII signal compared to WT (†, ††) and same genotype with in the presence of isoproterenol (ISO) (**). n=3. Statistical comparisons were performed using the Tukey-Kramer honestly significant difference test: †, $P<0.05$. ††, **, $P<0.01$. **B-C.** Effect of AIP on individual iPSC-CM membrane voltage and intracellular Ca^{2+}, as measured by Fluovolt and Rhod4 and confocal line scan imaging of isolated, single iPSC-CMs. Cells were preincubated for at least 10 minutes with or without AIP (300 nM), and then treated with ISO. B, Ca^{2+} sparks were recorded by confocal line scan imaging. Left, representative recordings. Right, quantification. C, Spontaneous changes in intracellular Ca^{2+} and membrane voltage in isolated, single iPSC-CMs, recorded by confocal line scan imaging. Left, representative Ca^{2+} and voltage tracings. Arrowheads indicate after-depolarizations and intracellular Ca^{2+} release events. Right, quantification. Steel-Dwass: †††, $P<0.001$. NS, not significant. Numbers by violin shapes indicate sample sizes.

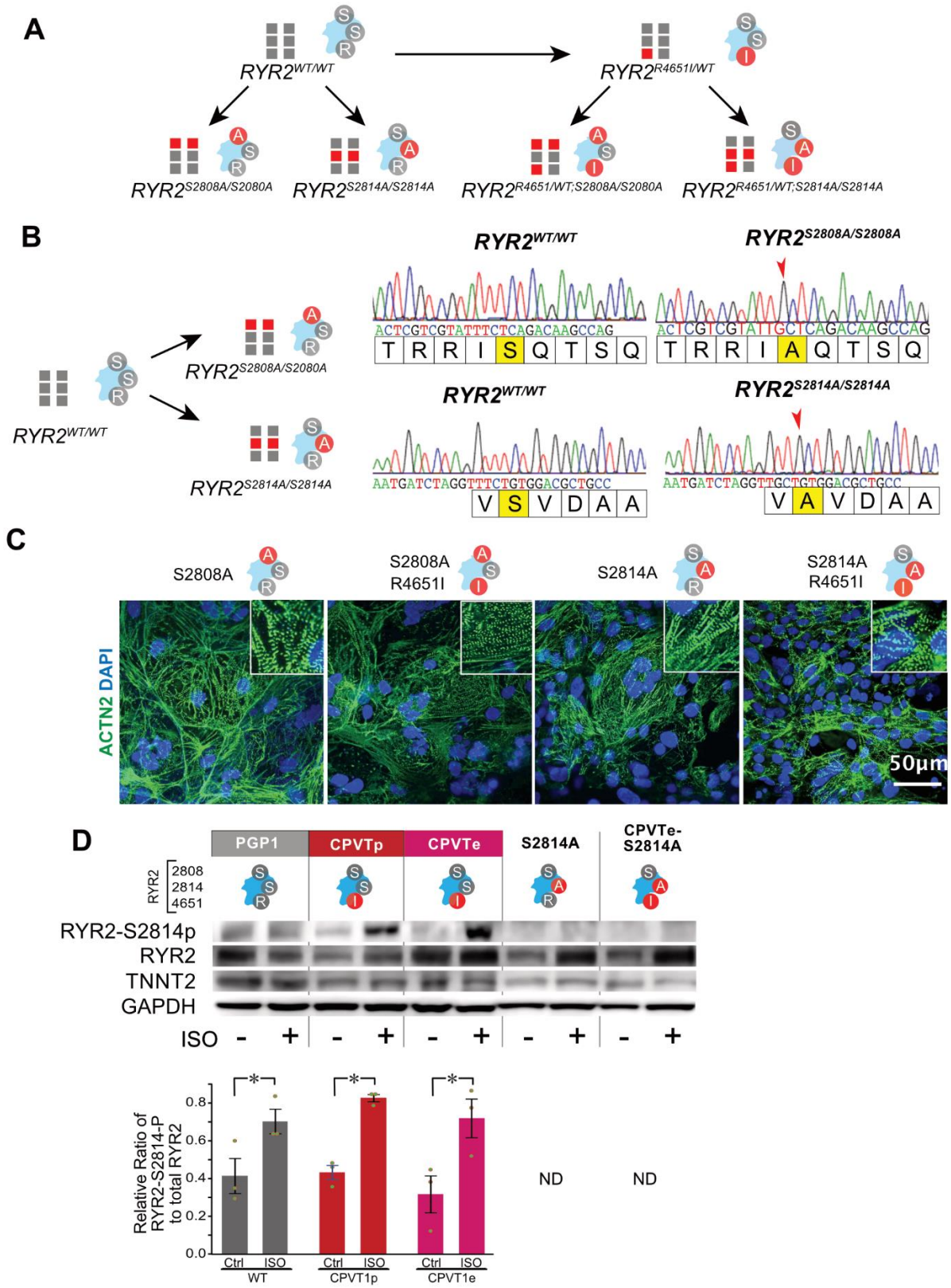

Supplementary Figure 19. Genome editing of S2808 and S2814 sites of RYR2. A. Genome editing strategy to obtain homozygous S2808A or S2814A mutations in either PGP1 (WT) or PGP1-RYR2$^{R4651I/+}$ (CPVT1e) iPSCs. **B.** Representative Sanger sequencing to confirm genome editing. **C.** iPSC-CM differentiation of genome edited cell lines. **D.** Western blots of indicated iPSC-CMs with and

without ISO treatment. RYR2-S2814 phosphorylation and total RYR2 were measured using specific antibodies. S2814A mutant cell lines did not exhibit detectable S2814 phosphorylation. ND, RYR2-S2814p was not detected. Quantitative analysis compared the RYR2-pS2814 to total RYR2 ratio of the indicated iPSC-CM line with and without ISO treatment. n=3. Student's *t*-test: *, $P<0.05$.

SUPPLEMENTAL REFERENCES

1. Wang G, Yang L, Grishin D, Rios X, Ye LY, Hu Y, Li K, Zhang D, Church GM, Pu WT. Efficient, footprint-free human iPSC genome editing by consolidation of Cas9/CRISPR and piggyBac technologies. *Nat Protoc*. 2017;12:88–103.

2. Ran FA, Ann Ran F, Hsu PD, Wright J, Agarwala V, Scott DA, Zhang F. Genome engineering using the CRISPR-Cas9 system. *Nat Protoc*. 2013;8:2281–2308.

3. Tohyama S, Hattori F, Sano M, Hishiki T, Nagahata Y, Matsuura T, Hashimoto H, Suzuki T, Yamashita H, Satoh Y, Egashira T, Seki T, Muraoka N, Yamakawa H, Ohgino Y, Tanaka T, Yoichi M, Yuasa S, Murata M, Suematsu M, Fukuda K. Distinct metabolic flow enables large-scale purification of mouse and human pluripotent stem cell-derived cardiomyocytes. *Cell Stem Cell*. 2013;12:127–137.

4. Feinberg AW, Feigel A, Shevkoplyas SS, Sheehy S, Whitesides GM, Parker KK. Muscular thin films for building actuators and powering devices. *Science*. 2007;317:1366–1370.

5. Feinberg AW, Alford PW, Jin H, Ripplinger CM, Werdich AA, Sheehy SP, Grosberg A, Parker KK. Controlling the contractile strength of engineered cardiac muscle by hierarchal tissue architecture. *Biomaterials*. 2012;33:5732–5741.

6. Park S-J, Gazzola M, Park KS, Park S, Di Santo V, Blevins EL, Lind JU, Campbell PH, Dauth S, Capulli AK, Pasqualini FS, Ahn S, Cho A, Yuan H, Maoz BM, Vijaykumar R, Choi J-W, Deisseroth K, Lauder GV, Mahadevan L, Parker KK. Phototactic guidance of a tissue-engineered soft-robotic ray. *Science*. 2016;353:158–162.

7. Dittgen T, Nimmerjahn A, Komai S, Licznerski P, Waters J, Margrie TW, Helmchen F, Denk W, Brecht M, Osten P. Lentivirus-based genetic manipulations of cortical neurons and their optical and electrophysiological monitoring in vivo. *Proc Natl Acad Sci U S A*. 2004;101:18206–18211.

8. Alford PW, Feinberg AW, Sheehy SP, Parker KK. Biohybrid thin films for measuring contractility in engineered cardiovascular muscle. *Biomaterials*. 2010;31:3613–3621.

9. McCain ML, Agarwal A, Nesmith HW, Nesmith AP, Parker KK. Micromolded gelatin hydrogels for extended culture of engineered cardiac tissues. *Biomaterials*. 2014;35:5462–5471.

Supplemental Video 1

Three-dimensional reconstruction of confocal images of ACTN2-stained opto-MTFs. Engineered CPVT1p tissue was aligned on micromolded gelatin substrate with 25 μm wide and 5 μm deep grooves and 4 μm gap. Blue, DAPI nuclei stain, and white, α-actinin.

Supplemental Video 2

Simultaneous recording of Ca^{2+} wave propagation and contraction in WT tissue. Ca^{2+} wavefront (top) and Ca^{2+} wave (bottom) initiated by local optical stimulation (1.5 Hz, 10 ms light pulses) at the left side of a WT opto-MTF propagated rightward toward two cantilevers, activating mechanical contraction that deflected the cantilevers. Ca^{2+} wavefront was calculated by the temporal derivative of the Ca^{2+} signal acquired by the Ca^{2+} imaging setup. Simultaneously, mechanical deflection of the two cantilevers (top right) was recorded by dark field imaging. The video plays at 0.5x real time. Scale bar, 2 mm.

Supplemental Video 3

Simultaneous recording of Ca^{2+} wave propagation and contraction in CPVT1p tissue. See caption to Supplemental Video 2 for details.

Supplemental Video 4

Independent stimulation of adjacent opto-MTFs. Four opto-MTFs engineered from neonatal rat ventricular cardiomyocytes were independently stimulated by local illumination at 1.5, 2, 3, and 4 Hz. Each opto-MTF, containing two film cantilevers, was cut and separated from adjacent MTFs, and each MTF has its own optical fiber for pacing. The cantilevers of each MTF are contracting 1:1 to the pacing stimulus. The video plays in real-time. Scale bar, 2 mm.

Supplemental Video 5

"Dancing" MTFs illustrate independent stimulation of adjacent opto-MTFs. Every two film cantilevers in four NRVM opto-MTFs were stimulated by light pulses synchronized to music. This demonstrates that the opto-MTFs can be independently controlled by using optical fiber to pace each opto-MTF.. The video plays in real-time.

Supplemental Video 6

WT opto-MTF with and without ISO and paced at 1.5 or 3 Hz. Representative WT hiPSC-CM opto-MTF retained organized Ca^{2+} wave propagation and synchronous 1:1 contraction in the absence or presence of 10 μM ISO challenge and at 1.5 or 3 Hz optical pacing. Ca^{2+} wavefronts (left) were calculated as the temporal derivative of Ca^{2+} signals acquired by the Ca^{2+} imaging setup. Simultaneously, the mechanical deflection of two cantilevers (right) was recorded by dark field imaging. The video play at 0.5x real time. Scale bar, 2 mm.

Supplemental Video 7

CPVT1p opto-MTF with and without ISO and paced at 1.5 or 3 Hz. Representative CPVT patient-derived hiPSC-CM opto-MTF retained organized Ca^{2+} wave propagation and synchronous contraction in the absence of ISO challenge and 1.5 Hz optical pacing. However, the CPVT1p opto-MTF developed spiral wave reentry and asynchronous contraction when challenged with 10 μM ISO and 3 Hz optical pacing. See Supplemental Video 6 caption for further details.

Supplemental Video 8

CPVT2e opto-MTF with and without ISO and paced at 1.5 or 3 Hz. Representative CPVT2e opto-MTF retained organized Ca^{2+} wave propagation in the absence of ISO challenge and 1.5 Hz optical pacing.

However, the CPVT2e opto-MTF developed spiral wave reentry when challenged with 3 Hz optical pacing. See Supplemental Video 6 caption for further details.

Supplemental Video 9

Sustained reentry in CPVT1e opto-MTF. CPVT1e opto-MTF treated with ISO developed reentry during 3 Hz pacing (top) that was sustained after cessation of pacing (bottom). See Supplemental Video 6 caption for further details.

Supplemental Video 10

CPVT1p opto-MTF showing Ca^{2+} wave propagation and contraction during rotor initiation by collision of paced and spontaneous Ca^{2+} waves. Two CPVT1p hiPSC-CM opto-MTFs developed spiral Ca^{2+} wave propagation, reentry, and asynchronous rapid low-amplitude contraction at 1.5 Hz optical pacing and without ISO, via the collision of pacing-driven Ca^{2+} waves with spontaneous Ca^{2+} waves. Ca^{2+} wavefronts (left) were calculated by the temporal derivative of Ca^{2+} signals acquired by the Ca^{2+} imaging setup. Simultaneously, the mechanical deflection of two cantilevers (right) was recorded by dark field imaging. The video plays at 0.5x real time. Scale bar, 1 mm.

Supplemental Video 11

CPVT1e opto-MTF paced at 3 Hz, showing disorganized Ca^{2+} wave propagation and time-varying Ca^{2+} activation map. Heterogeneous Ca^{2+} wave propagation containing retrograde Ca^{2+} wave propagation developed across the multiple pulses. Ca^{2+} wavefronts (top) were calculated by the temporal derivative of Ca^{2+} signals acquired by the Ca^{2+} imaging setup. Each Ca^{2+} activation map (bottom) was calculated by identifying the time with the maximum upstroke slope. The video plays at 0.2x real time. Scale bar, 1 mm.

Supplemental Video 12

Same CPVT1e opto-MTF as Supplemental Video 11, paced at 2 Hz, showing well-ordered Ca^{2+} wave propagation and time-invariant Ca^{2+} activation map. Ca^{2+} wavefronts (top) were calculated by the temporal derivative of Ca^{2+} signals acquired by Ca^{2+} imaging setup. Each Ca^{2+} activation map (bottom) was calculated by identifying the time with the maximum upstroke slope. The video plays at 0.2x real time. Scale bar, 1 mm.

Supplemental Video 13

Rotor initiation in CPVT1p opto-MTF paced at 3 Hz. Heterogeneous Ca^{2+} wave propagation developed with 3 Hz pacing (pulse #1) with ISO. As high frequency pacing proceeded, the Ca^{2+} wave propagation became more dispersed (pulse #10 to #18), which induced conduction block (pulse #18 and #19) and eventually reentrant Ca^{2+} propagation (pulse #19). At the initiation of reentry, the core of reentry was located at the point where conduction block appeared for the first time, and then moved toward the middle of the engineered tissue with subsequent pacing pulses (pulse #20 and #21). Ca^{2+} wavefronts (top) were calculated by the temporal derivative of Ca^{2+} signals acquired by the Ca^{2+} imaging setup. Each Ca^{2+} activation map (bottom) was calculated by identifying the time with the maximum upstroke slope. The video plays at 0.2x real time. Scale bar, 1 mm.

Supplemental Video 14

Same CPVT1p opto-MTF as Supplemental Video 13, paced at 2 Hz, showing well-ordered Ca^{2+} wave propagation and time-invariant Ca^{2+} activation map. Unlike 3 Hz pacing, at 2 Hz pacing the same CPVT1p opto-MTF of Supplemental Video 11 retained organized Ca^{2+} wave propagation across 17 consecutive optical pulses. Ca^{2+} wavefronts (top) were calculated by the temporal derivative of Ca^{2+}

signals acquired by the Ca^{2+} imaging setup. Each Ca^{2+} activation map (bottom) was calculated by identifying the time with the maximum upstroke slope. The video plays at 0.2x real time. Scale bar, 1 mm.

Supplemental Video 15

Rotor initiation in CPVT1e opto-MTF paced at 2.5 Hz. Similar with the reentry formation of CPVT1p opto-MTF (Supplemental Video XI), CPVT1e opto-MTF initiated rotor (pulse #3) via heterogeneous Ca^{2+} propagation (pulse #1) and following instant conduction block (pulse #2). The core of reentry was located at the point where conduction block appeared for the first time, and then moved toward the middle of the engineered tissue with subsequent pacing pulses (pulse #4 to #15). Ca^{2+} wavefronts (top) were calculated by the temporal derivative of Ca^{2+} signals acquired by Ca^{2+} imaging setup. Each Ca^{2+} activation map (bottom) was calculated by identifying the time with the maximum upstroke slope. The video plays at 0.2x real time. Scale bar, 1 mm.

Supplemental Video 16

Same CPVT1e opto-MTF as Supplemental Video 15, paced at 2 Hz, showing well-ordered Ca^{2+} wave propagation and Ca^{2+} activation map. Unlike 2.5 Hz pacing, at 2 Hz pacing the same CPVT1e opto-MTF wtih Supplemental Video 14 retained organized Ca^{2+} wave propagation across 10 consecutive optical pulses. Ca^{2+} wavefronts (top) were calculated by the temporal derivative of Ca^{2+} signals acquired by Ca^{2+} imaging setup. Each Ca^{2+} activation map (bottom) was calculated by identifying the time with the maximum upstroke slope. The video plays at 0.2x real time. Scale bar, 1 mm.

Supplemental Video 17

CPVT1e opto-MTF treated with AIP, a CaMKII inhibitor, with and without ISO and paced at 2 Hz. CaMKII inhibition stopped reentry formation in CPVT1e tissue. Ca^{2+} wavefronts were calculated by the temporal derivative of Ca^{2+} signals acquired by the Ca^{2+} imaging setup. The video plays at 0.5x real time. Scale bar, 2 mm.

Supplemental Video 18

CPVT1e-S2814A opto-MTFs with and without ISO and paced at 1.5 or 3 Hz. Representative CPVT1e-S2814A hiPSC-CM opto-MTF with the deletion of CaMKII phosphorylation site of RYR2 retained organized Ca^{2+} wave propagation and synchronous contraction in the absence or presence of 10 μM ISO challenge and at 1.5 or 3 Hz optogenetic pacing, unlike CPVTp opto-MTF. Ca^{2+} wavefronts (left) were calculated by the temporal derivative of Ca^{2+} signals acquired by the Ca^{2+} imaging setup. Simultaneously, the mechanical deflection of two cantilevers (right) was recorded by dark field imaging. The video plays at 0.5x real time. Scale bar, 2 mm.